Search for Higgs bosons produced via vector-boson fusion and decaying into bottom quark pairs in $\sqrt{s} = 13$ TeV pp collisions with the ATLAS detector

M. Aaboud *et al.**
(ATLAS Collaboration)

A search for the $b\bar{b}$ decay of the Standard Model Higgs boson produced through vector-boson fusion is presented. Three mutually exclusive channels are considered: two all-hadronic channels and a photon-associated channel. Results are reported from the analysis of up to 30.6 fb^{-1} of pp data at $\sqrt{s} = 13$ TeV collected with the ATLAS detector at the LHC. The measured signal strength relative to the Standard Model prediction from the combined analysis is $2.5^{+1.4}_{-1.3}$ for inclusive Higgs boson production and $3.0^{+1.7}_{-1.6}$ for vector-boson fusion production only.

I. INTRODUCTION

Following the discovery of a new particle with a mass of 125 GeV by the ATLAS and CMS Collaborations at the Large Hadron Collider (LHC) [1,2], there has been an extensive effort to measure its properties and compare them with theoretical predictions for the Standard Model (SM) Higgs boson [3–9]. Precise measurements of the Higgs boson couplings to other SM particles provide insight into the nature of electroweak symmetry breaking since the values of the couplings are determined by the underlying symmetry-breaking mechanism. The SM Higgs boson production rates and branching ratios are determined by the values of these couplings, and deviations from the predicted values may indicate new particles or forces beyond the Standard Model. The dominant decay of the SM Higgs boson is into $b\bar{b}$, but the measurement of Higgs bosons in this decay mode is challenging because the dominant production mechanisms—gluon-gluon fusion (ggF) and vector-boson fusion (VBF)—yield leading-order final states containing only jets. These hadronic final states are difficult to distinguish from nonresonant b-quark production, which has a much larger production rate. Most previous measurements of $H \rightarrow b\bar{b}$ decays were made with the relatively rare process of Higgs boson production in association with a leptonically decaying vector boson (VH, where V denotes a W or Z boson). The combined result for a Higgs boson with a mass of

125 GeV from the CDF and D0 experiments is a signal strength $\mu = \sigma/\sigma_{SM} = 1.9 \pm 0.8$ with a 2.8σ signal significance [10]. This was followed by measurements with higher significance from ATLAS of $\mu = 0.90 \pm 0.27$ at 3.6σ [11] and CMS of $\mu = 1.1 \pm 0.3$ at 3.8σ [12].

The VBF process, $pp \rightarrow qqH$, in which the Higgs boson is accompanied by two light-flavor quarks separated by a large rapidity gap, provides a striking experimental signature for distinguishing Higgs boson production from backgrounds. A measurement of $H \rightarrow b\bar{b}$ decay in VBF production mode provides information that is complementary to the measurement in VH production mode. The expected production rate $\sigma_{VBF} \times B(H \rightarrow b\bar{b})$ is 2.2 pb [13–19] at the center-of-mass energy $\sqrt{s} = 13$ TeV. Using data collected at $\sqrt{s} = 8$ TeV and corresponding to an integrated luminosity of 20.2 fb^{-1}, the ATLAS experiment set a 95% confidence level (C.L.) limit on the production rate of 4.4 times the expected production rate from a VBF-dominated sample with a signal strength $\mu = -0.8 \pm 2.3$ times the predicted value [20]. The CMS Collaboration used approximately 20 fb^{-1} of 8 TeV data to measure a signal strength $\mu = 2.8^{+1.6}_{-1.4}$ corresponding to an observed significance of 2.2σ [21].

This article reports the results from a set of complementary search channels sensitive to SM Higgs boson production through VBF with decay into $b\bar{b}$. Two of the search channels focus on the process $qqH(\rightarrow b\bar{b})$ [Fig. 1(a)] with central and forward jets. They are collectively referred to as the *all-hadronic* channels because their event selection uses jets only. The third channel focuses on Higgs boson production in association with a high-momentum photon, $qqH(\rightarrow b\bar{b})\gamma$ [Fig. 1(b)] and is referred to as the *photon* channel. The presence of an associated photon suppresses the gluon-rich dominant

---

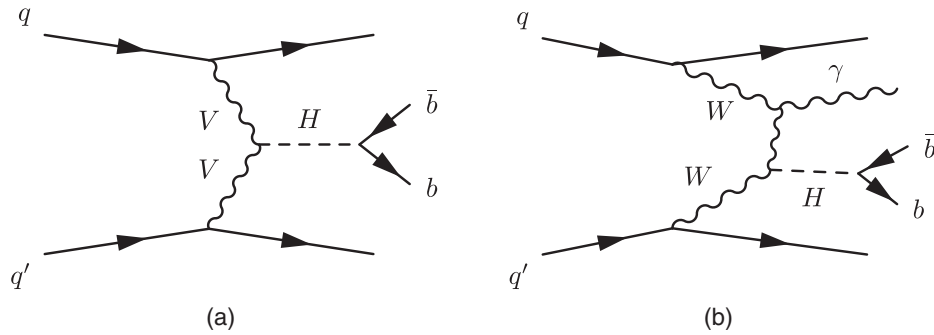*Full author list given at the end of the article.

FIG. 1.   Representative Feynman diagrams for Higgs boson production via vector-boson fusion (a) without and (b) with an associated photon. The photon in the right-hand figure may be radiated from any quark leg or charged vector boson.

non-resonant $b\bar{b}jj$ background [22,23], further increasing the sensitivity to the VBF final state. This channel was not included in any previous VBF results.

In all three channels, the signal events are characterized by two central b-jets from the decay of a Higgs boson and two light-quark jets with a large rapidity gap between them (VBF jets). Kinematic properties of the events are used as inputs to boosted decision trees (BDT) trained to classify events as signal-like or backgroundlike. Backgrounds include contributions from nonresonant jet pairs and from resonant production of Z bosons. The signal is extracted from a simultaneous fit to the di-b-jet invariant mass (m_{bb}) distribution in several regions defined by the BDT discriminant output value. Nonresonant $b\bar{b}jj$ background and $Z\,(+\gamma)$ + jets background are estimated separately from the fit in each signal region. Both the inclusive Higgs boson production and the VBF production are measured and presented. The all-hadronic channels are sensitive to ggF as well as VBF, but the photon channel is sensitive to VBF only.

II. ATLAS DETECTOR

ATLAS [24] is a multipurpose particle detector with a forward-backward symmetric cylindrical geometry and nearly 4π coverage in solid angle.[1] The interaction point is surrounded by inner tracking devices, a calorimeter system, and a muon spectrometer.

The inner detector provides precision tracking of charged particles for pseudorapidities $|\eta| < 2.5$ and is surrounded by a superconducting solenoid providing a 2 T magnetic field. The inner detector consists of silicon pixel and microstrip detectors and a transition radiation tracker.

---

[1]ATLAS uses a right-handed coordinate system with its origin at the nominal interaction point (IP) in the center of the detector and the z axis along the beam pipe. The x axis points from the IP to the center of the LHC ring, and the y axis points upward. Cylindrical coordinates (r, ϕ) are used in the transverse plane, ϕ being the azimuthal angle around the beam pipe. The pseudorapidity is defined in terms of the polar angle θ as $\eta = -\ln\tan(\theta/2)$.

One significant upgrade for the $\sqrt{s} = 13$ TeV run is the insertable B-layer [25], an additional pixel layer close to the interaction point. It provides high-resolution hits at a small radius to improve tracking performance.

In the pseudorapidity region $|\eta| < 3.2$, high-granularity lead/liquid-argon (LAr) electromagnetic (EM) sampling calorimeters are used to measure EM showers from photons and electrons. An iron/scintillator tile calorimeter measures hadron energies for $|\eta| < 1.7$. The endcap and forward regions, spanning $1.5 < |\eta| < 4.9$, are also instrumented with LAr calorimeters for both the EM and hadronic measurements.

The muon spectrometer consists of a large barrel and two endcap superconducting toroid magnets with eight coils each, a system of trigger chambers, and precision tracking chambers providing triggering and tracking capabilities for muons in the ranges $|\eta| < 2.4$ and $|\eta| < 2.7$, respectively.

A two-level trigger system selects events. The first-level trigger (L1), implemented in hardware, is followed by the software-based high-level trigger, which runs offline reconstruction and calibration software reducing the event rate to less than 1 kHz.

III. SIGNAL AND BACKGROUND SIMULATION

Simulated events are used for signal modeling, BDT training, and background shape determination. The signal models include both the Higgs boson VBF and ggF production contributions, as well as the small contribution from associated production with top quarks ($t\bar{t}H$) and vector bosons (VH). Simulated all-hadronic signal events were generated at next-to-leading order in QCD with POWHEG-BOX V2 [26–28], using the CT10 parton distribution functions (PDFs) [29] and PYTHIA 8.212 [30] for parton showering and fragmentation with the AZNLO tuned parameter set [31]. Contributions from VH and $t\bar{t}H$ production were modeled with PYTHIA 8.212, using the NNPDF PDF [32], and with MADGRAPH5_aMC@NLO V2.2.2 [33] showered with Herwig++ 2.7.1 [34] and using the NLO CT10 PDF, respectively. Simulated Z + jets events from strong and electroweak production were

generated separately at leading order (LO) plus two partons with MADGRAPH5_aMC@NLO V2.2.3 using the NNPDF PDFs and interfaced to PYTHIA 8.205 with the A14 set of tuned parameters [35] for the underlying-event description. The nonresonant backgrounds in the all-hadronic channels are derived exclusively from the data.

In the photon channel, both the $jj\gamma b\bar{b}$ final-state signal and background events were generated at LO with MADGRAPH35_aMC@NLO V2.3.3 using the PDF4LHC_ nlo_mc PDFs [36] and interfaced to PYTHIA 8.212 with the A14 tuned parameter set. The VH and $t\bar{t}H$ signals were modeled using the same samples as the all-hadronic channels. Background events containing two b-quarks from the decay of a Z boson, a photon, and two additional jets were generated separately for strong and electroweak processes. Nonresonant γ + jets simulation events were generated by requiring the same final state as the signal and $Z + \gamma$ background events but excluding diagrams containing on-shell Higgs or Z bosons. The nonresonant γ + jets simulation sample is only used in BDT training, while the nonresonant background shape and normalization are obtained from a fit to the m_{bb} data distribution in signal regions (Sec. IX).

Multiple pp collisions were simulated with the soft QCD processes of PYTHIA 8.186 [37] using the A2 tuned parameter set [38] and the MSTW2008LO PDFs [39]. These additional interactions were overlaid on the hard-scatter interaction of the signal and background samples according to the luminosity profile of the recorded data to model contributions from pp interactions in both the same bunch crossing and neighboring bunch crossings (pileup). The response of the ATLAS detector to the generated events was then modeled using full simulation software [40] based on GEANT 4 [41], except for the $Z(b\bar{b})$ + jets events, which were passed through a fast simulation where the full calorimeter simulation is replaced by a parametrization of shower shapes [42].

IV. DATA SETS AND OBJECT RECONSTRUCTION

This analysis uses LHC pp collision data at a center-of-mass energy of 13 TeV collected between September 2015 and October 2016. The data set corresponds to an integrated luminosity of 24.5 fb^{-1} for the all-hadronic channels and 30.6 fb^{-1} for the photon channel. The difference in luminosity between the channels is due to limited availability of the triggers for the all-hadronic channels during some periods of the data-taking. The trigger requirements are described in Sec. V. Detector quality requirements are applied to ensure that the selected events are well measured. Events are selected using the properties of jets and photons that are reconstructed as described briefly below.

Jets are reconstructed from topological calorimeter-cell clusters calibrated to the EM scale. These clusters are inputs to the anti-k_t jet reconstruction algorithm [43] with a radius parameter of $R = 0.4$. A likelihood-based discriminant, the jet vertex tagger [44], is applied to jets with transverse momenta $p_T < 60$ GeV and $|\eta| < 2.4$ to suppress jets originating from pileup vertices. The energy of a jet is corrected using scale factors derived from both the simulated events and an *in situ*, data-based calibration [45] comparing the p_T balance between a jet and a reference object, such as a Z boson, a photon, or a multijet system for various jet-p_T ranges. In addition, a pileup subtraction algorithm is applied to reduce pileup contributions to the calorimeter-based jet energy.

A flavor-tagging algorithm MV2c10 [46,47] tags jets containing b-hadrons within the acceptance of the inner detector ($|\eta| < 2.5$) using log-likelihood ratios from three-dimensional impact parameter significance distributions, secondary vertex information, and the jet p_T and η. This information is input to a BDT that calculates the final discriminant. Three different flavor-tagging operating points are used, corresponding to b-tagging efficiencies of 70%, 77%, and 85%, respectively, as measured in simulated $t\bar{t}$ events for jets having $p_T > 20$ GeV and $|\eta| < 2.5$ [48]. The c-jet misidentification efficiencies are measured to be 8.2%, 16%, and 32%, respectively, and the light jet misidentification efficiencies are measured to be 0.3%, 0.7%, and 3.0%, respectively. Scale factors are applied to each selected b-tagged jet to account for the b-, c- and light-jet flavor-tagging performance differences between data and simulation. Because the invariant mass m_{bb} is an important discriminant against the nonresonant background, additional energy corrections are applied to b-jets after the jet selection and generic energy calibration. These additional corrections account for semileptonic decays and resolution effects such as energy losses outside of the jet cone [11]. After these corrections, the full width at half maximum for the signal dijet invariant mass distribution, m_{bb}, is 22 GeV for the all-hadronic channels and 27 GeV for the photon channel. The difference is due to the different kinematic requirements for the jets.

Photon reconstruction [49] is seeded from clusters of energy deposits in the electromagnetic calorimeter. The initial selection based on *loose* criteria uses shower shapes in the second layer of the electromagnetic calorimeter and the energy deposits in the hadronic calorimeter. The *tight* identification adds information from the finely segmented first layer of the calorimeter, which provides good rejection of hadronic jets in which a neutral meson carries most of the jet energy. Clusters without any matching track or conversion vertex are classified as unconverted photon candidates. Clusters with a matching vertex reconstructed from one or two tracks are converted photon candidates. Both the converted and unconverted photon candidates with transverse energy $E_T > 30$ GeV in the pseudorapidity ranges $|\eta| < 1.37$ or $1.52 < |\eta| < 2.37$ are used. The range $1.37 < |\eta| < 1.52$ is excluded because it is the gap between the barrel and endcap sections of the calorimeter. To further suppress hadronic background from jets and neutral pions,

an isolation requirement is applied to the photon candidates. The calorimeter isolation variable E_T^{iso} is the sum of the transverse energy of three-dimensional positive-energy topological clusters [50] reconstructed in the electromagnetic and hadronic calorimeters in a cone of size $\Delta R \equiv \sqrt{(\Delta\phi)^2 + (\Delta\eta)^2} = 0.4$ around the photon candidate, where the $\Delta\eta \times \Delta\phi$ region of size 0.125×0.175 around the photon cluster's centroid is excluded. The isolation requirement, which depends explicitly on the photon transverse energy E_T^γ, is $E_T^{iso} < 2.45$ GeV $+ 0.022 \times E_T^\gamma$. This requirement provides a signal efficiency around 98% over the E_T range expected for the photon channel.

Electrons are reconstructed [51] with a sliding-window algorithm based on the clusters of energy deposits in the electromagnetic calorimeter and matched to the tracks from the inner detector. Electron candidates must satisfy the *tight* likelihood-based electron identification criteria [52], which combine the requirements of calorimeter shower shape, track-to-cluster association, and associated track qualities. Identified electrons are required to pass track- and calorimeter-based isolation requirements and to have $E_T > 27$ GeV and $|\eta| < 2.47$. The track-based isolation requirement is a function of the electron p_T and is based on the other tracks around the electron-associated track within a variable cone size up to $\Delta R = 0.2$. The calorimeter-based isolation criterion requires the sum of transverse energies of clusters not associated with an electron candidate within a cone of $\Delta R = 0.2$ around the electron track to be smaller than 3.5 GeV.

Muons are reconstructed [53] by combining the inner detector and muon spectrometer measurements up to $|\eta| = 2.5$. Muon candidates are required to have $p_T > 25$ GeV and satisfy the *medium* muon identification criteria [53]. Identified muons must pass an isolation selection requiring the sum of transverse momenta of tracks within a cone of $\Delta R = 0.2$ around the muon track, excluding the muon candidate, to be smaller than 1.25 GeV.

Double-counting of photons, leptons, and jets is avoided by applying an overlap removal algorithm based on the ΔR distance metric. First, jets within $\Delta R = 0.2$ of any identified photons, muons or electrons are removed. Then, any photons, muons and electrons that lie $0.2 < \Delta R < 0.4$ from the jet axis are removed. Finally, photons within $\Delta R = 0.4$ of an identified muon are removed, and electrons within $\Delta R = 0.4$ of an identified photon are removed.

V. EVENT SELECTION

The event selection targets three distinct final-state topologies: two all-hadronic channels and the photon channel. The selection criteria are matched to a set of dedicated trigger algorithms used to identify events compatible with VBF $H \to b\bar{b}$ production. In the following, the central region corresponds to $|\eta| < 2.8$, and the forward

regions correspond to the range $3.2 < |\eta| < 4.4$. The channel definitions are as follows:

(i) two-central: at least one VBF jet is required to be in the forward region, and both b-tagged jets from the Higgs boson decay are in the central region,

(ii) four-central: both VBF jets and both b-tagged jets from the Higgs boson decay are found in the central region of the detector, and

(iii) photon: a photon and both b-tagged jets from the Higgs boson decay are found in the central region and both VBF jets are within the detector acceptance.

The selected events for the two all-hadronic channels are mutually exclusive. The small overlap between the photon and all-hadronic channels is removed with an explicit veto of any data events in the all-hadronic selection passing the photon selection. The 0.5% overlap in the simulated signal sample is ignored.

A. Two-central channel trigger and event selection

The two-central channel requires a central jet with $E_T > 40$ GeV, another central jet with $E_T > 25$ GeV, and a forward jet with $E_T > 20$ GeV to pass the L1 trigger.

In the high-level trigger, one central b-tagged jet [54] at the 70% b-tagging efficiency working point with $E_T > 80$ GeV, another central b-tagged jet at the 85% b-tagging efficiency working point with $E_T > 60$ GeV, and a forward jet with E_T at least 45 GeV are required. The same b-tagging algorithm is used in the online selection as in the offline selection.

Selected events must have at least four offline reconstructed jets with $p_T > 20$ GeV and $|\eta| < 4.4$. Among the selected jets, at least one jet must have $p_T > 95$ GeV, have $|\eta| < 2.4$, and pass the 70% b-tagging efficiency working point requirement. The $|\eta|$ requirement is narrower than the nominal requirement for b-tagging ($|\eta| < 2.5$) for comparison with a supporting trigger used for validation. At least one additional jet is required to pass the 85% b-tagging efficiency working point selection and have $p_T > 70$ GeV and $|\eta| < 2.5$. Finally, events are required to have at least one forward jet with $p_T > 60$ GeV. These thresholds were determined by the efficiency plateau of the trigger-jet transverse-energy requirements. The two highest-p_T b-tagged jets are chosen to form the Higgs boson candidate. Among the remaining jets, the two jets with highest invariant mass including at least one forward jet are designated as the VBF jets.

B. Four-central channel trigger and event selection

The four-central channel requires four central jets to pass the L1 trigger with $E_T > 15$ GeV.

The requirements of the high-level trigger varied during the course of data-taking. In the first half, events were required to have two b-tagged jets with $E_T > 45$ GeV passing the 70% efficiency working point requirements for the trigger b-tagging algorithm. In the second half, the

trigger's jet E_T thresholds were changed to 35 GeV and the b-tagging algorithm was tightened to operate at 60% efficiency to achieve an overall lower rate of events passing the high-level trigger.

The selected events are required to have at least four jets reconstructed with offline algorithms with $p_T > 55$ GeV and $|\eta| < 2.8$ to match the trigger requirements. At least two jets must pass the 70% b-tagging efficiency working point requirement. All b-tagged jets must be within the acceptance of the inner detector ($|\eta| < 2.5$). The two highest-p_T b-tagged jets form the Higgs boson candidate. Among the remaining jets, the pair of non-b-tagged jets with highest invariant mass is taken as the VBF jet pair. Finally, events containing at least one forward jet with $p_T > 60$ GeV are removed to avoid overlap with the two-central channel.

C. Photon channel trigger and event selection

The photon channel requires a photon to pass the L1 trigger with $E_T > 22$ GeV. In the high-level trigger, a photon with $E_T > 25$ GeV is required in addition to at least four jets with $E_T > 35$ GeV and $|\eta| < 4.9$, and at least

one dijet pair with invariant mass greater than 700 GeV. For the first half of the data-taking, no online b-tagging requirements were applied; for the second half, which had increased instantaneous luminosity, at least one jet is required to be b-tagged at the 77% efficiency working point.

The event selection for the photon channel requires a photon with $E_T > 30$ GeV in the calorimeter regions $|\eta| < 1.37$ or $1.52 < |\eta| < 2.37$. Events must have at least four jets, all satisfying $p_T > 40$ GeV and $|\eta| < 4.4$, with at least two jets in $|\eta| < 2.5$ passing the 77% b-tagging efficiency working point requirement. The two highest-p_T b-tagged jets are taken to be the signal jets of the Higgs boson decay. Among the remaining jets, the pair with the highest invariant mass is chosen to be the VBF jet pair. The invariant mass of the VBF jets is required to be at least 800 GeV so that the trigger requirement imposed on the invariant mass is fully efficient.

D. The bb-system p_T requirement

The jet p_T thresholds in the trigger and the offline selection sculpt the m_{bb} distribution. To remove this sculpting, which could bias the final m_{bb} fit, the bb-system p_T in

TABLE I.   Trigger and event selection criteria for all search channels. L1 and HLT refer to the first-level trigger and the high-level trigger, respectively. The p_T and $|\eta|$ requirements on the offline jets are used to match trigger selections and flavor-tagging requirements. All the selection criteria are applied independently.

Two-central channel		
Trigger	L1	≥ 2 central jets with $E_T > 40, 25$ GeV ≥ 1 forward jet with $E_T > 20$ GeV
	HLT	≥ 2 central b-jets at 70%, 85% efficiency working points with $E_T > 80, 60$ GeV ≥ 1 forward jet with $E_T > 45$ GeV
Offline		≥ 2 b-jets at 70%, 85% efficiency working points with $p_T > 95, 70$ GeV and $|\eta| < 2.5$ ≥ 1 jet with $p_T > 60$ GeV and $3.2 < |\eta| < 4.4$ ≥ 1 jet with $p_T > 20$ GeV and $|\eta| < 4.4$ $p_T(bb) > 160$ GeV
Four-central channel		
Trigger	L1	≥ 4 central jets with $E_T > 15$ GeV
	HLT	≥ 2 central b-jets at 70% (or 60%) efficiency working point with $E_T > 45$ GeV (or 35 GeV)
Offline		≥ 2 b-jets at 70% efficiency working point with $p_T > 55$ GeV and $|\eta| < 2.5$ ≥ 2 jets with $p_T > 55$ GeV and $|\eta| < 2.8$ No jet with $p_T > 60$ GeV and $3.2 < |\eta| < 4.4$ $p_T(bb) > 150$ GeV
Photon channel		
Trigger	L1	≥ 1 photon with $E_T > 22$ GeV
	HLT	≥ 1 photon with $E_T > 25$ GeV ≥ 4 jets (or ≥ 3 jets and ≥ 1 b-jet at 77% efficiency working point) with $E_T > 35$ GeV and $|\eta| < 4.9$ $m_{jj} > 700$ GeV
Offline		≥ 1 photon with $E_T > 30$ GeV and $|\eta| < 1.37$ or $1.52 < |\eta| < 2.37$ ≥ 2 b-jets at 77% efficiency working point with $p_T > 40$ GeV and $|\eta| < 2.5$ ≥ 2 jets with $p_T > 40$ GeV and $|\eta| < 4.4$ $m_{jj} > 800$ GeV $p_T(bb) > 80$ GeV

the two-central, four-central, and photon channels is required to be larger than 150, 160, and 80 GeV, respectively.

The full event selection, including the trigger requirements and offline requirements, is summarized in Table I.

VI. MULTIVARIATE ANALYSIS

After the event selection requirements are applied, a set of BDTs classify events as being signal-like or background-like [55,56]. A separate BDT is trained for each channel with the AdaBoost [57] algorithm. Each BDT discriminant is constructed from a set of variables to maximize the separation between the signal and the dominant backgrounds. The discriminant is then used to define event categories of varying signal purity.

Since the observed signal is extracted from the m_{bb} spectrum, the input variables for each BDT are chosen to have low correlation with the bb invariant mass to prevent sculpting of the distribution. The number of input variables is minimized by excluding variables that give only marginal performance improvement. The following input variables are used for all channels, with $j1$ and $j2$ denoting the leading and sub-leading p_T VBF jets and with $b1$ and $b2$ denoting leading and subleading p_T Higgs boson b-jet candidates:

  (i) m_{jj}: the invariant mass of the VBF jet pair.
  (ii) p_T^{jj}: the transverse momentum of the VBF jet pair.
  (iii) N_{trk}^{j1}, N_{trk}^{j2}: the number of tracks with $p_T > 0.5$ GeV in the VBF jets, $j1$ and $j2$. This variable discriminates between gluon jets, which are more abundant in the background processes, and light-quark jets, which are present in the signal. The variable is only used for jets with $|\eta| < 2.5$.
  (iv) $p_T^{balance}$: the ratio of the vectorial and scalar sums of the jet (and photon, if applicable) transverse momenta,

$$\frac{|\vec{p}_T(j1) + \vec{p}_T(j2) + \vec{p}_T(b1) + \vec{p}_T(b2)|}{p_T(j1) + p_T(j2) + p_T(b1) + p_T(b2)}.$$

This variable discriminates between electroweak signal processes, which typically are balanced, and multijet QCD events, which are less balanced.
  (v) $\cos\theta$: cosine of the angle between the normal directions of the planes spanned by the VBF jet pair and signal b-jet pair in the center-of-mass frame of the $jjbb$ system, which is related to the angular dynamics of the production mechanism.

In addition to these common variables, the two-central and four-central channel BDTs include the following input variables:

  (i) $\max(\eta) \equiv \max(|\eta_{j1}|, |\eta_{j2}|)$: the maximum absolute value of the VBF jet pseudorapidity.
  (ii) $\eta^* = \frac{1}{2}(|\eta_{j1}| + |\eta_{j2}| - |\eta_{b1}| - |\eta_{b2}|)$: the average pseudorapidity difference between VBF and signal jets. This variable discriminates between QCD multijet events, which have no average pseudorapidity

difference, and VBF processes, where the VBF jets are on average more forward than the signal jets.
  (iii) $\min \Delta R(j1)$: minimum angular separation between the leading VBF jet and the closest jet with $p_T > 20$ GeV and $|\eta| < 4.4$ which is not a signal or VBF jet.
  (iv) $\min \Delta R(j2)$: minimum angular separation between the subleading VBF jet and the closest jet with $p_T > 20$ GeV and $|\eta| < 4.4$ which is not a signal or VBF jet.
  (v) Δm_{jj}: the difference between the invariant mass of the VBF jet pair and the largest invariant mass of any jet pair in the event, excluding the two jets forming the Higgs boson candidate.

The photon channel BDT includes the following variables in addition to the common variables:

  (i) $\Delta R(b1, \gamma)$, $\Delta R(b2, \gamma)$: angular separation between the signal b-jets and the photon.
  (ii) $\Delta\eta_{jj}$: η separation between the VBF jets.
  (iii) centrality(γ, jj): centrality of the photon relative to the VBF jets:

$$\text{centrality}(\gamma, jj) = \left| \frac{y_\gamma - \frac{y_{j1} + y_{j2}}{2}}{y_{j1} - y_{j2}} \right|,$$

    where y is the rapidity.
  (iv) $\Delta\phi(bb, jj)$: azimuthal angle between the VBF jet pair and the signal b-jet pair.

The training signal samples are the VBF signal simulation samples described in Sec. III. For the two-central and four-central channel BDTs, the training background sample is a set of data events in the mass sidebands 80 GeV $< m_{bb} < 100$ GeV and 150 GeV $< m_{bb} < 190$ GeV. Events from $Z + $ jets production are not removed; however, they contribute 2(3)% to the low mass sideband for the two (four)-central channel. Because data from the sidebands are used as the training sample for the hadronic channels, a three-fold validation of the BDT training is performed to verify possible overtraining. The signal and background samples are randomly divided into three equal subsets which are then each used to train the BDT while the other two subsets are used for testing. Equal discriminating power is found across all subsets. The effect of potential bias on the m_{bb} distribution from overtraining was checked by repeating the analysis in the training and validation sets. Additionally, Asimov data sets were produced by reweighting the sidebands to the observed difference in the ratio of events in the training and validation samples for each region. Observed biases in these tests were negligible compared to the total statistical error on the signal. In the photon channel, there are not enough data events to form a training sample, so the nonresonant $\gamma + $ jets simulation sample is used as the background training sample. The entire set of events is split into two samples for training and evaluation. To validate the modeling of the nonresonant
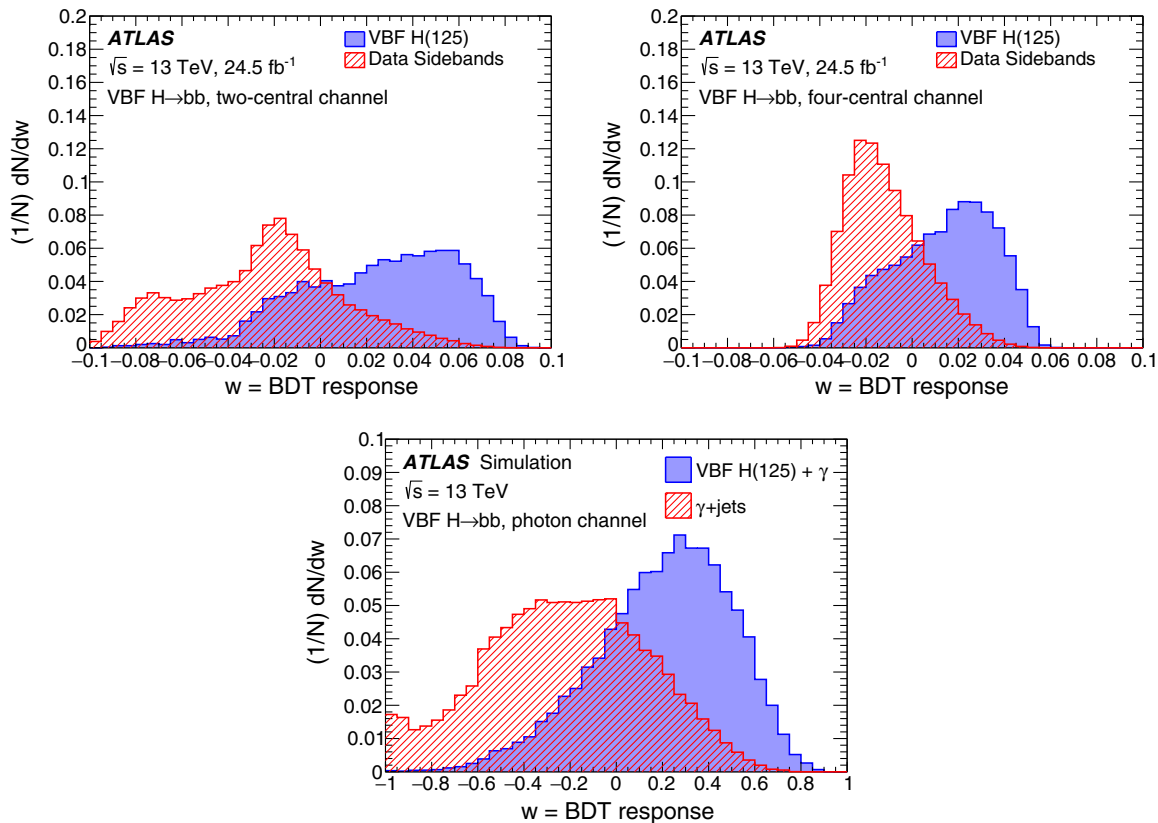
FIG. 2. The BDT response w for the signal and dominant backgrounds, normalized to unity. The two-central channel is on the top left, the four-central channel is on the top right, and the photon channel is shown in the bottom row. For these plots, the background refers to the continuum background derived either from the m_{bb} sidebands in data (all-hadronic channels) or from the $\gamma +$ jets simulation sample (photon channel).

QCD background, the simulated events are compared with the data events in the mass sidebands ($m_{bb} < 100$ GeV and $m_{bb} > 140$ GeV). Correction functions are applied to reweight some of the kinematic distributions [$\Delta\eta_{jj}$, p_T^{jj}, p_T^{balance}, and minimum of $\Delta R(b1, \gamma)$ and $\Delta R(b2, \gamma)$] to improve the overall modeling by the nonresonant QCD simulation sample. The reweighting process is performed iteratively. The correction function is determined for the kinematic distribution of one of the input variables. This function is then applied back to the nonresonant $\gamma +$ jets simulation sample to reweight the kinematic distribution of the input variable that the correction function is determined for. At the same time, the kinematic distributions of other input variables correlated with this input variable also show improved agreement with the data after the reweighting. The distributions of the other uncorrelated

input variables are not affected by the reweighting. The process is repeated to reweight the other three kinematic variables.

The BDT responses for the signal and background samples are shown in Fig. 2. The output discriminant from each BDT is used to define several signal regions (SR). The two-central channel has two regions, the four-central has four regions, and the photon channel has three regions as summarized in Table II. The four-central channel does not include the full BDT range in the set of signal regions because including events with lower BDT response did not improve the significance of the result. These region definitions are optimized for sensitivity to the Higgs boson signal while limiting the maximum experimental uncertainty of the Z boson contribution in any signal region to less than 1.5 times the Standard Model Z boson prediction.

TABLE II. Criteria for the BDT responses used to define the signal regions (SR) for the three channels.

Region	SR IV	SR III	SR II	SR I
Four-central	(0.002, 0.015]	(0.015, 0.026]	(0.026, 0.033]	> 0.033
Two-central			< -0.006	≥ -0.006
Photon		< -0.05	[-0.05, 0.30]	> 0.30

The requirement on the precision of the Z boson contribution is necessary because this contribution is a parameter in the fit and the signal regions must be large enough to ensure it is well measured.

VII. BACKGROUND AND SIGNAL MODELING

The main sources of background contributing to the final-state signatures are divided into two groups: processes with decay of a massive particle into b-tagged jet pairs and processes with nonresonant b-tagged jet pairs. The resonant backgrounds are dominated by $Z(+\gamma) + $ jets, with small contributions from $W(+\gamma) + $ jets. The nonresonant backgrounds are dominated by multijet $(+\gamma)$ production, with small contributions from $t\bar{t}$ $(+\gamma)$ and single-top events. For all of the backgrounds, b-tagged jets may correspond to true b-jets or to misidentified c-jets, τ-jets, or light-flavor jets. Both the background and signal m_{bb} shapes are parametrized with functions that are derived differently depending on whether they arise from a resonant or nonresonant process. The contributions from $Z(+\gamma) + $ jets and multijet $(+\gamma)$ production background processes are derived from fits to the m_{bb} data distribution using template distributions or analytical functions constructed from sideband data regions or simulation samples. The contributions from other background processes are estimated from simulations.

The Higgs boson and $Z \to b\bar{b}$ resonance shapes are parametrized with histogrammed Bukin functions [58] (two-central and four-central channels) or Crystal Ball functions [59,60] (photon channel). In general, the m_{bb} distributions are well modeled by these functions, and a closure test performed on a representative test data set, called an Asimov data set [61], composed of these distributions plus the nonresonant background indicates no bias in the extracted signal normalization.

In all channels, the nonresonant background distributions are modeled as polynomials and derived from data. In the two-central and four-central channels, Bernstein polynomials are fit to the sidebands of the m_{bb} distribution outside the signal region of 100 GeV $< m_{bb} < 140$ GeV for each BDT region separately. The photon channel uses a general polynomial. The $Z + $ jets contribution is subtracted using predictions from simulations; tests showed that subtracting twice the prediction does not change the chosen

function. For all channels, the lowest-order polynomial which satisfies basic goodness-of-fit requirements, including χ^2 and F tests, is chosen as a candidate. Using Asimov data sets derived from alternative background parametrizations which also satisfy these criteria in fits to the data sidebands, an additional function-selection criterion is applied to ensure that the chosen function candidate does not create any significant spurious signal. This criterion is that any function which induces a spurious Higgs boson signal contribution with an absolute signal strength of one or larger in these Asimov data sets is discarded. This requirement minimizes the possibility that the chosen function could generate a signal. The alternative functions used include a product of Bernstein polynomials and exponential functions, as well as a sum of exponential functions. A third-order Bernstein polynomial is the lowest-order polynomial which satisfies these criteria for the two-central and four-central channel regions, except SR IV of the four-central channel, which requires a fourth-order Bernstein polynomial. The photon channel uses a second-order polynomial.

The $Z(\to b\bar{b}) + $ jets contribution plays an important role in the fit procedure because it contributes to the low m_{bb} sideband and affects the continuum background determination. Studies have shown that typical methods of estimating uncertainties for a leading-order $Z + $ jets simulation may not be appropriate in the regions of phase space used in this analysis, including high-p_{T} boson production with widely separated jets [62]. Therefore, its normalization is allowed to float independently in each BDT region. In the two-central and four-central channels, the low mass sideband extends only to 80 GeV due to the trigger thresholds. Therefore, it does not provide a strong constraint on the $Z(\to b\bar{b}) + $ jets contribution, and consequently the determination of this background contributes significantly to the overall uncertainty. In the photon channel, the sidebands extend to 50 GeV, allowing the fit to provide a strong constraint on the $Z(\to b\bar{b}) + $ jets contribution.

A summary of the estimated number of signal events in the Higgs boson mass window of 100 GeV $< m_{bb} <$ 140 GeV is given in Table III. There is up to a 60% contribution of ggF events to the Higgs boson signal in the all-hadronic channels in the least sensitive signal regions and up to a 20% contribution in the photon channel.

TABLE III.   Expected numbers of signal events within the Higgs boson mass window of 100 GeV $< m_{bb} < 140$ GeV estimated from simulations. Statistical uncertainties are shown for the predictions from simulations.

Channel	Two-central		Four-central				Photon		
Region	SR I	SR II	SR I	SR II	SR III	SR IV	SR I	SR II	SR III
VBF	101.2 ± 2.0	22.2 ± 0.9	51.6 ± 1.1	28.4 ± 0.9	43.1 ± 1.0	41.9 ± 1.1	6.2 ± 0.1	5.5 ± 0.1	2.3 ± 0.1
ggF	23.8 ± 2.6	75.7 ± 6.1	11.3 ± 2.2	13.2 ± 1.5	43.4 ± 3.8	127.0 ± 6.5	0.5 ± 0.2	0.3 ± 0.1	0.8 ± 0.3
VH	0.2 ± 0.2	6.0 ± 1.2	1.2 ± 0.9	0.7 ± 0.3	3.9 ± 0.8	28.9 ± 2.6	< 0.1	< 0.1	< 0.1
$t\bar{t}H$	2.0 ± 0.2	14.6 ± 0.7	0.3 ± 0.1	1.0 ± 0.1	5.7 ± 0.3	20.2 ± 0.5	< 0.1	< 0.1	0.4 ± 0.1

VIII. SYSTEMATIC UNCERTAINTIES

The systematic uncertainties for the background and signal expectations are divided into experimental and theoretical uncertainties. The uncertainties discussed below affect only the simulation-based signal and background predictions. They do not affect the nonresonant background estimates because those estimates are derived from data. All uncertainties are propagated to the BDT input variables and then to the final likelihood fits, with the exception of the luminosity uncertainty, which is taken as a constant uncertainty. In the likelihood fits for signal extraction, the uncertainties affect the m_{bb} spectrum modeling and normalization of signal processes in each region, as well as the m_{bb} spectrum modeling of the Z boson background. The impact of the uncertainties on the BDT output and m_{bb} shape are determined together and fully correlated. Uncertainties from sources common to the signal and Z boson background are treated as correlated between the two.

A. Experimental uncertainties

The uncertainty in the integrated luminosity is 2.2% for the all-hadronic channels and 2.1% for the photon channel with the difference due to the small difference in luminosity between the channels. It is derived, following a methodology similar to that detailed in Ref. [63] from a calibration of the luminosity scale using x–y beam-separation scans performed in August 2015 and May 2016. This systematic uncertainty is applied to all physics processes estimated with simulation samples.

The most prominent sources of jet-related uncertainty are the uncertainties in the jet energy scale (JES) and jet energy resolution (JER). The JES uncertainty is determined primarily by using Z, photon, and multijet p_T-balancing techniques in data [45]. The per-jet uncertainty in the energy scale varies from approximately 1% to 5% for the jets considered in this analysis. The systematic uncertainties of the additional energy corrections specific to b-jets are found to be negligible.

The JER uncertainties are also determined *in situ* via Z, photon, and dijet p_T -balancing techniques [45]. The systematic uncertainty due to the JER is calculated by increasing the resolution within its uncertainties, smearing the jet energy by the resulting change in resolution, and comparing the result to the nominal shape and normalization in simulation. The signal mass resolution varies by 3% to 4% due to the systematic uncertainty in the jet energy resolution.

The uncertainties related to the b-tagging of jets are implemented as variations of simulation correction factors (scale factors). These scale factors and their associated uncertainties are determined from data using $t\bar{t}$ events, $W + c$ and D^* events, and multijet data [46,47]. The systematic uncertainties for each jet are propagated to a total event uncertainty. To simplify the computation and reduce the number of significant uncertainties, a principal-component analysis is performed over all of the contributing uncertainties to generate a reduced set of nuisance parameters. For b-jets, the uncertainty is approximately 2%, while it is 10% for c-jets and 30% for light jets. Scale factors for the online b-tagging algorithms and their uncertainties are derived relative to the offline algorithms and applied to b-jets. The uncertainties are typically 2%–5%.

The uncertainty due to the jet vertex tagging requirement is measured in $Z(\to \ell^+\ell^-) + 1$-jet events. The uncertainty per event is less than 2% [44].

To estimate the effects of uncertainties in the number of tracks associated with a jet, tracks are removed or added according to the tracking efficiency and fake-rate estimates [64]. Uncertainties in the modeling of track multiplicity are derived from the measurement of the charged-particle multiplicity inside jets from $\sqrt{s} = 8$ TeV pp collisions [65]. These effects lead to an uncertainty in the average number of charged particles associated with the jet of approximately 10%.

In the photon channel, the analysis is not highly sensitive to photon energy uncertainties, so multiple sources of electromagnetic energy scale and resolution uncertainties are combined into a set of just two parameters. The uncertainties were derived from calibration studies in data and data to simulation comparisons [66,67]. A data-driven correction is applied to account for a shift between the data and simulation distributions of the photon isolation energy. The difference between the uncorrected and corrected isolation energy is taken as a systematic uncertainty.

Systematic uncertainties from electrons and muons are negligible and hence are neglected.

B. Theoretical uncertainties

The value of the $H \to b\bar{b}$ branching ratio and its uncertainty are from the recommendations of the LHC Higgs Cross Section Working Group for $m_H = 125$ GeV [68] and are calculated by the HDECAY program [14]. Uncertainties in the cross section and acceptance for VBF and ggF signals due to the missing higher-order terms in perturbative QCD calculations are evaluated by varying the choice of renormalization scale and factorization scale independently by factors of 0.5 and 2.0. Specific uncertainties are applied for ggF events with additional radiation which generates a VBF-like topology. The ggF events are classified as VBF-like if they have at least two additional jets with an invariant mass greater than 400 GeV. The uncertainties in the cross section are approximately 20% in this phase space. The total cross-section and acceptance uncertainties affect the signal yields by 4–15% in the all-hadronic channels and 10%–16% in the photon channel. Uncertainties in the cross section and acceptance due to the choice of PDF are evaluated by varying the error eigenvectors of the nominal PDFs. They result in 5%–10% uncertainties in the signal yields.

The uncertainty from the parton-shower and underlying-event models is estimated by comparing the nominal sample, which uses PYTHIA 8.2 for parton showering, with an alternative sample using HERWIG 7.0 for parton-shower generation. This uncertainty is 4%–12%. These uncertainties are also propagated to the m_{bb} shape.

The contributions of the VH and $t\bar{t}H$ Higgs boson production modes to the all-hadronic channels' signal regions are small in the most sensitive signal regions (0.2%–3%) and rise to 20% in the least sensitive regions. The contribution from these processes is included in the total Higgs boson yield, and 100% uncertainty is taken for their relative contribution. In the photon analysis the ggF and $t\bar{t}H$ contributions are small, and 100% uncertainty is assumed. The yield from these processes is added to the Higgs boson yields from VBF and VH processes.

C. Nonresonant and *Z* boson background uncertainties

The uncertainty due to the nonresonant background modeling is included by determining the largest spurious signal induced in Asimov data sets derived with alternative functions which describe the data sidebands equally well. These alternative functions must pass the χ^2 and F-test as described in Sec. VII. The size of the spurious signal is taken as the uncertainty and is typically 20%–30% of the expected Higgs boson signal. This uncertainty is included in the total experimental uncertainties.

The uncertainties due to the Z boson background fall into two categories. Experimental uncertainties in the observed Z boson resonance shape are determined as described in Sec. VIII A. Normalization uncertainties are determined from the fit.

IX. FITS FOR HIGGS BOSON PRODUCTION

The inclusive Higgs boson signal strength μ_H and the VBF-specific strength μ_{VBF} are extracted from an extended maximum-likelihood fit to the b-tagged dijet invariant mass spectrum m_{bb} in data. The two-central and four-central channels use a joint binned likelihood fit with a bin size of 0.5 GeV. The signal strength is common to the two channels. The photon channel, which has fewer events, uses an unbinned fit to maximize the sensitivity. The fit range is 80 GeV $< m_{bb} <$ 200 GeV for the two-central and four-central channels and 50 GeV $< m_{bb} <$ 250 GeV for the photon channel. The different lower mass bounds for the two fits is because the photon channel has lower jet thresholds. For the two-central and four-central channel fits, there is no benefit to extending the fit range beyond an m_{bb} of 200 GeV.

In all cases, the likelihood is built from the product of Poisson probability terms across all channels and BDT regions with three contributions: nonresonant background, Z boson events, and Higgs boson signal events. The parametrization of these contributions is described in Sec. VII. The likelihood includes terms for systematic uncertainties implemented as nuisance parameters. The nuisance parameters describe the systematic uncertainties discussed in Sec. VIII and are parametrized by Gaussian or log-normal priors. Each prior constrains a nuisance parameter to its nominal value within its associated uncertainty.

The strength of the Higgs boson signal, either inclusive or VBF-specific, is the parameter of interest. Other free parameters include the shape parameters of the nonresonant background and the normalizations of the nonresonant and Z boson backgrounds in each region. Signal-injection tests confirmed the linearity of the fit with no bias. The
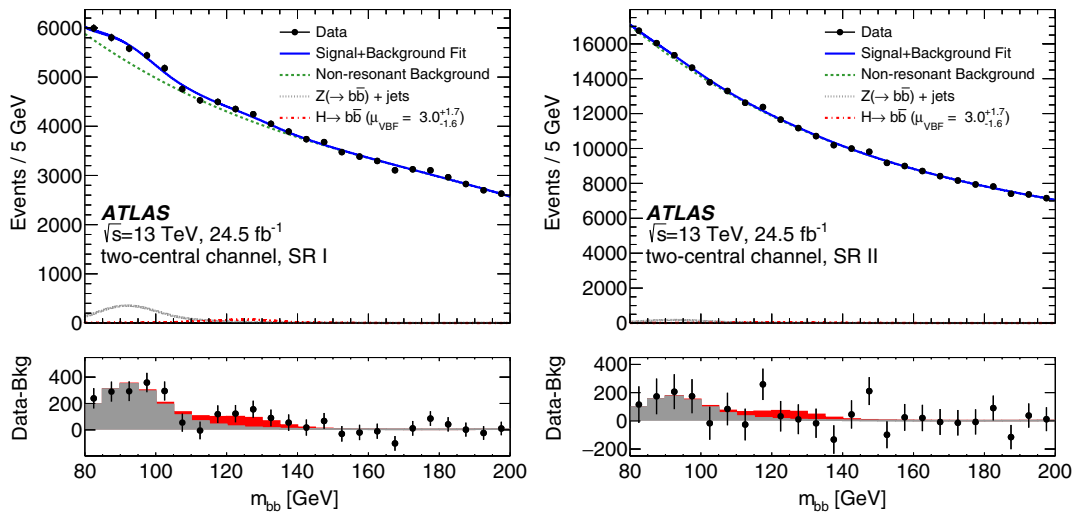

FIG. 3.   Data and fit model comparison for the combined profile likelihood fit for μ_{VBF} in the two-central channel signal regions. The combined fit includes all signal regions for the all-hadronic and photon channels. The fitted continuum background is shown with a dashed green line, the fitted Z boson background with a dotted gray line, and the fitted Higgs boson signal with a dash-dotted red line. The total fit is displayed with a solid blue line. The bottom panels show the residuals of the data relative to the continuum background fit, along with the simulated Z boson background and Higgs boson signal normalized to the fitted signal strengths. Only statistical uncertainties are shown.

all-hadronic and photon results are also combined in a simultaneous likelihood fit with the signal strength treated as correlated across all analysis regions. In the case of the inclusive extraction of μ_H, all production mechanisms (VBF, ggF, VH, and $t\bar{t}H$) are considered as signal, and their ratios are fixed to the SM predictions. In the case of the VBF-only extraction of μ_{VBF}, all channels include the contributions of ggF, $t\bar{t}H$, and VH as nuisance parameters constrained to their Standard Model expectations with the uncertainties described in Sec. VIII B.

With the exception of the b-tagging uncertainties, the experimental uncertainties are treated as fully correlated between the channels. The b-tagging uncertainties for both the offline and online algorithms are taken as fully uncorrelated between different working points. Treating them as correlated or uncorrelated has no impact on the

overall result or uncertainty. Theoretical uncertainties, including those in the QCD scale of the VBF process, the parton showering, the PDFs, and the $t\bar{t}H$ yield, are correlated. In general, background systematic uncertainties such as nonresonant background normalization/parametrization, Z boson normalization, and spurious signals are specific to each channel and consequently not correlated. Systematic uncertainties related to the fit procedure are characterized by spurious-signal nuisance parameters. These are treated as uncorrelated across the signal regions.

The m_{bb} invariant mass distributions after the combined μ_{VBF} fits are shown in Figs. 3–5 for each region and each channel. The Higgs boson signal, Z boson background, and nonresonant background yields in the Higgs boson mass window of 100 GeV $< m_{bb} <$ 140 GeV after performing the combined fit are shown in Table IV.

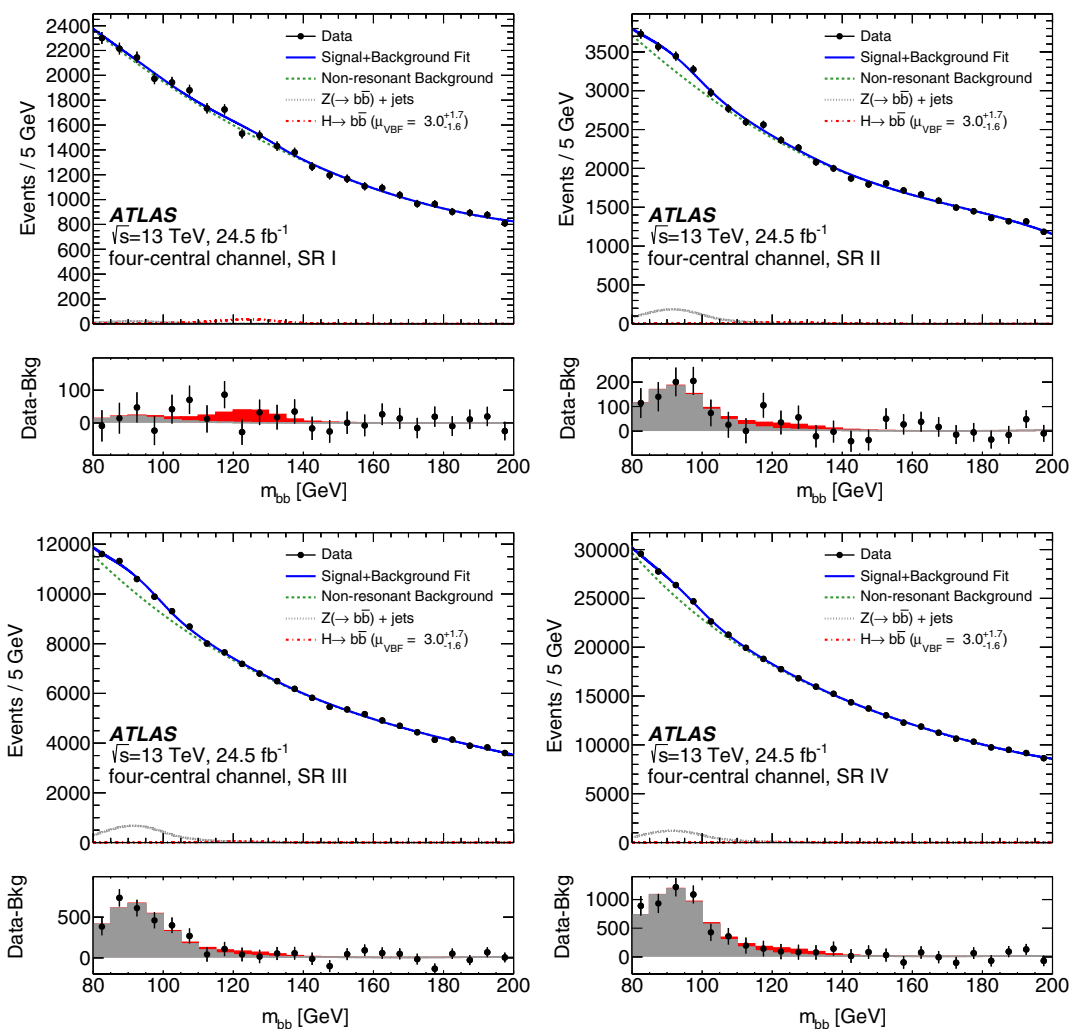FIG. 4. Data and fit model comparison for the combined profile likelihood fit for μ_{VBF} in the four-central channel signal regions. The combined fit includes all signal regions for the all-hadronic and photon channels. The fitted continuum background is shown with a dashed green line, the fitted Z boson background with a dotted gray line, and the fitted Higgs boson signal with a dash-dotted red line. The total fit is displayed with a solid blue line. The bottom panels show the residuals of the data relative to the continuum background fit, along with the simulated Z boson background and Higgs boson signal normalized to the fitted signal strengths. Only statistical uncertainties are shown.

FIG. 5.   Data and fit model comparison for the combined profile likelihood fit for μ_{VBF} in the photon channel signal regions. The combined fit includes all signal regions for the all-hadronic and photon channels. The fitted continuum background is shown with a dashed green line, the fitted Z boson background with a dotted gray line, and the fitted Higgs boson signal with a dash-dotted red line. The total fit is displayed with a solid blue line. The bottom panels show the residuals of the data relative to the continuum background fit, along with the simulated Z boson background and Higgs boson signal normalized to the fitted signal strengths. Only statistical uncertainties are shown.
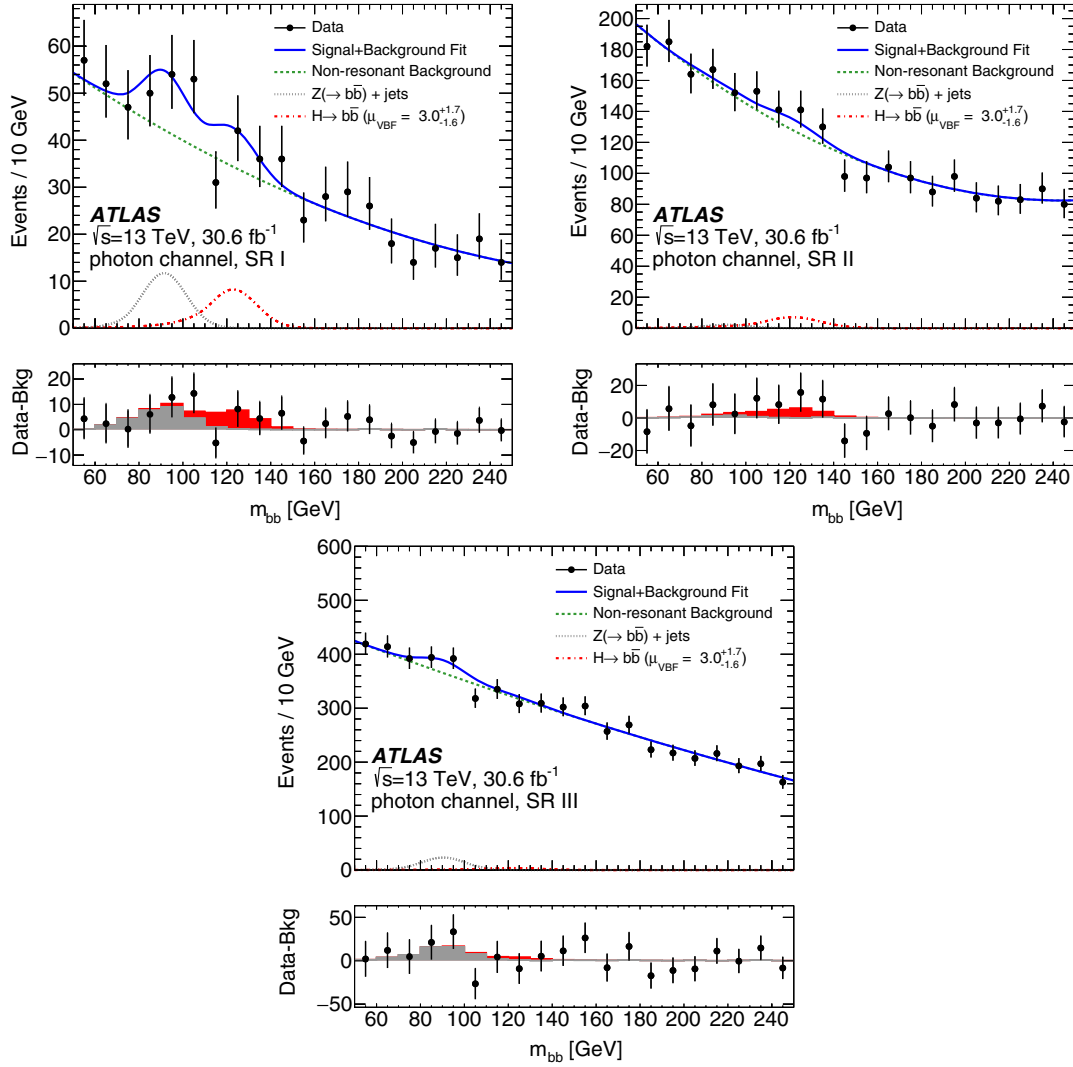
A test statistic based on the profile likelihood function is used to determine the probability that the data set is compatible with the Higgs boson signal hypothesis. Distributions of the test statistic under the signal and null (background-only) hypotheses are estimated using asymptotic approximations [61]. As no statistically significant signal is observed, the $\mathrm{CL_s}$ technique [69] is used to derive 95% C.L. upper limits on $H \to b\bar{b}$ production in both the

TABLE IV.   Numbers of signal, background, and data events within the Higgs boson mass window of 100 GeV $< m_{bb} <$ 140 GeV. Signal and background yields are derived from the combined fit for the extraction of μ_{VBF}. Uncertainties include both the statistical and systematic uncertainties.

Channel	Two-central		Four-central				Photon		
Region	SR I	SR II	SR I	SR II	SR III	SR IV	SR I	SR II	SR III
Higgs boson	340^{+120}_{-130}	165^{+50}_{-29}	167^{+60}_{-58}	101^{+40}_{-21}	183^{+50}_{-46}	304^{+100}_{-51}	$21.1^{+7.7}_{-7.1}$	$20.1^{+9.5}_{-7.2}$	$10.6^{+7.8}_{-4.1}$
Z + jets ($Z\gamma$)	470^{+140}_{-180}	230^{+210}_{-230}	22^{+80}_{-22}	197^{+90}_{-95}	720^{+190}_{-180}	$1,260^{+270}_{-250}$	$5.8^{+3.3}_{-3.6}$	$1.1^{+5.8}_{-1.1}$	$9.8^{+7.8}_{-7.9}$
Nonresonant background	$34,620^{+310}_{-280}$	$95,620^{+420}_{-420}$	$12,870^{+150}_{-190}$	$19,340^{+200}_{-240}$	$59,340^{+340}_{-340}$	$146,930^{+630}_{-510}$	$140.4^{+6.1}_{-6.8}$	518^{+10}_{-13}	$1,296^{+18}_{-19}$
Data	35,496	95,802	13,139	19,611	60,314	148,413	162	565	1,270

TABLE V. Expected and observed results for the Higgs boson production rate, for both inclusive production and VBF production only, relative to the Standard Model prediction. Where the results are reported by channel, the fit is performed with that channel only. The limits shown refer to 95% C.L. upper limits.

Results	Inclusive production			VBF production		
	All-hadronic	Photon	Combined	All-hadronic	Photon	Combined
Expected significance	0.5σ	0.6σ	0.8σ	0.4σ	0.6σ	0.7σ
Observed significance	1.4σ	1.3σ	1.9σ	1.4σ	1.4σ	1.9σ
Expected limit on signal strength	$4.1^{+1.9}_{-1.2}$	$3.4^{+1.5}_{-1.0}$	$2.5^{+1.0}_{-0.7}$	$5.9^{+2.6}_{-1.7}$	$3.7^{+1.6}_{-1.0}$	$3.0^{+1.3}_{-0.8}$
Observed limit on signal strength	6.8	5.5	4.8	9.7	6.1	5.9
Expected signal strength	1.0 ± 1.9	1.0 ± 1.7	1.0 ± 1.2	1.0 ± 2.8	1.0 ± 1.8	1.0 ± 1.5
Observed signal strength	$2.7^{+2.2}_{-2.0}$	$2.3^{+1.9}_{-1.7}$	$2.5^{+1.4}_{-1.3}$	$4.1^{+3.2}_{-2.9}$	$2.5^{+2.0}_{-1.9}$	$3.0^{+1.7}_{-1.6}$

TABLE VI. Uncertainties and their effects on the Higgs boson signal strength in the combined fit for both the inclusive production (μ_H) and VBF-only production (μ_{VBF}). The combined fit includes all signal regions for the all-hadronic channels and photon channel. Uncertainties are grouped into statistical and systematic uncertainties.

Uncertainty	$\sigma(\mu_H)$	$\sigma(\mu_{\mathrm{VBF}})$
Total statistical uncertainty	$+1.3 - 1.3$	$+1.6 - 1.5$
Data statistical uncertainty	$+0.6 - 0.6$	$+0.9 - 0.9$
Nonresonant background	$+1.0 - 1.0$	$+1.2 - 1.2$
$Z + \mathrm{jets}$ normalization	$+0.5 - 0.5$	$+0.5 - 0.5$
Total systematic uncertainty	$+0.6 - 0.4$	$+0.6 - 0.5$
Higgs boson modeling	$+0.3 - 0.1$	$+0.2 - 0.1$
JES/JER	$+0.3 - 0.2$	$+0.4 - 0.2$
b-tagging (including trigger)	$+0.2 - 0.1$	$+0.2 - 0.1$
Other experimental uncertainty	$+0.4 - 0.3$	$+0.4 - 0.4$
Total	$+1.4 - 1.3$	$+1.7 - 1.6$

inclusive and VBF channels. The likelihood fit results for the Higgs boson normalization are shown in Table V, both for the individual channels and for the combined fits. The results are consistent with Standard Model expectations within the uncertainties. A summary of the uncertainties is shown in Table VI. The effect of data statistical uncertainty on the

Higgs signal strength is derived by fixing all nuisance parameters to their best-fit values and taking the differences between the central value and the 1σ interval for the measured Higgs signal strength. The effect from nonresonant background parameters is then derived as the difference in quadrature between the uncertainty effects on the Higgs signal strength derived by floating and fixing the corresponding nuisance parameters. A similar procedure is performed to calculate the impact of the other uncertainties. The total uncertainty is dominated by statistical uncertainties, with important contributions from the determination of the nonresonant background parameters and Z normalization due to the weak constraining power of the low m_{bb} sideband. The experimental systematic uncertainties, as defined in Sec. VIII A, also contribute significantly to the total uncertainty. Of these, the leading uncertainties are due to the JES and JER uncertainties, followed by b-tagging uncertainties. The spurious signal contributes an uncertainty of less than 0.1 for both the individual and combined signal extractions.

The results for the extraction of μ_H and μ_{VBF} are also shown in Table V and displayed in Fig. 6. The observed significances and signal strengths are higher than the expected significances for all channels. The observed significances of both the inclusive and VBF-only production are 1.9σ, compared with 0.8σ expected for the
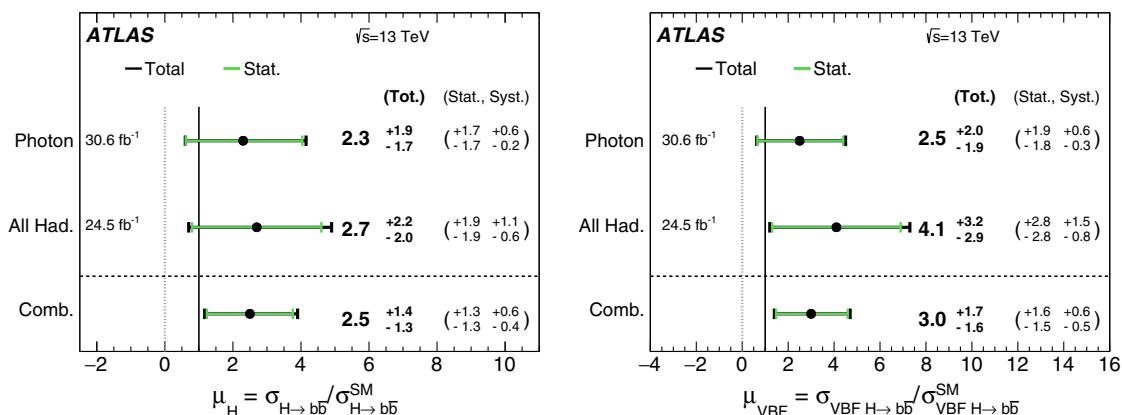

FIG. 6. Summary of the all-hadronic, photon, and combined results for the fitted signal strength parameters μ_H (left) and μ_{VBF} (right). The inner error bars show the statistical uncertainties. The outer error bars show the total uncertainties.

inclusive production and 0.7σ expected for the VBF production. The observed signal strength, μ_H, is $2.5^{+1.4}_{-1.3}$ for inclusive production, as compared with 1.0 ± 1.2 expected. For VBF production, μ_{VBF} is observed to be $3.0^{+1.7}_{-1.6}$, which can be compared with an expectation of 1 ± 1.5.

X. CONCLUSIONS

A search is presented for the Standard Model Higgs bosons produced through vector-boson fusion and decaying into $b\bar{b}$ using three distinct event signatures including production with an associated photon. The results use up to 30.6 fb^{-1} of LHC pp data at $\sqrt{s} = 13$ TeV collected with the ATLAS detector.

The combined observed (expected) 95% C.L. upper limits on the Higgs boson production cross section times branching ratio are 4.8 ($2.5^{+1.0}_{-0.7}$) times the Standard Model expectation for inclusive production, and 5.9 ($3.0^{+1.3}_{-0.8}$) times the Standard Model expectation for VBF production.

The measured Higgs boson signal strength relative to the Standard Model prediction μ_H for the three channels combined is $2.5^{+1.4}_{-1.3}$. The combined VBF-only signal strength μ_{VBF} is $3.0^{+1.7}_{-1.6}$.

[1] ATLAS Collaboration, Observation of a new particle in the search for the Standard Model Higgs boson with the ATLAS detector at the LHC, Phys. Lett. B **716**, 1 (2012).

[2] CMS Collaboration, Observation of a new boson at a mass of 125 GeV with the CMS experiment at the LHC, Phys. Lett. B **716**, 30 (2012).

[3] ATLAS Collaboration, Evidence for the spin-0 nature of the Higgs boson using ATLAS data, Phys. Lett. B **726**, 120 (2013).

[4] ATLAS Collaboration, Study of the spin and parity of the Higgs boson in diboson decays with the ATLAS detector, Eur. Phys. J. C **75**, 476 (2015); Erratum, Eur. Phys. J. C **76**, 152 (2016).

[5] ATLAS Collaboration, Measurements of the Total and Differential Higgs Boson Production Cross Sections Combining the $H \rightarrow \gamma\gamma$ and $H \rightarrow ZZ^* \rightarrow 4\ell$ Decay Channels at $\sqrt{s} = 8$ TeV with the ATLAS Detector, Phys. Rev. Lett. **115**, 091801 (2015).

[6] ATLAS and CMS Collaborations, Measurements of the Higgs boson production and decay rates and constraints on its couplings from a combined ATLAS and CMS analysis of the LHC pp collision data at $\sqrt{s} = 7$ and 8 TeV, J. High Energy Phys. 08 (2016) 045.

[7] CMS Collaboration, Measurement of differential cross sections for Higgs boson production in the diphoton decay channel in pp collisions at $\sqrt{s} = 8$ TeV, Eur. Phys. J. C **76**, 13 (2016).

[8] CMS Collaboration, Measurement of differential and integrated fiducial cross sections for Higgs boson production in the four-lepton decay channel in pp collisions at $\sqrt{s} = 7$ and 8 TeV, J. High Energy Phys. 04 (2016) 005.

[9] CMS Collaboration, Measurements of properties of the Higgs boson decaying into the four-lepton final state in pp collisions at $\sqrt{s} = 13$ TeV, J. High Energy Phys. 11 (2017) 047.

[10] CDF and D0 Collaborations, Evidence for a Particle Produced in Association with Weak Bosons and Decaying to a Bottom-Antibottom Quark Pair in Higgs Boson Searches at the Tevatron, Phys. Rev. Lett. **109,** 071804 (2012).

[11] ATLAS Collaboration, Evidence for the $H \to b\bar{b}$ decay with the ATLAS detector, J. High Energy Phys. 12 (2017) 024.

[12] CMS Collaboration, Evidence for the Higgs boson decay to a bottom quark–antiquark pair, Phys. Lett. B **780,** 501 (2018).

[13] T. Han, G. Valencia, and S. Willenbrock, Structure Function Approach to Vector Boson Scattering in pp Collisions, Phys. Rev. Lett. **69,** 3274 (1992).

[14] A. Djouadi, J. Kalinowski, and M. Spira, HDECAY: A program for Higgs boson decays in the Standard Model and its supersymmetric extension, Comput. Phys. Commun. **108,** 56 (1998).

[15] K. Arnold et al., VBFNLO: A Parton level Monte Carlo for processes with electroweak bosons, Comput. Phys. Commun. **180,** 1661 (2009).

[16] P. Bolzoni, F. Maltoni, S.-O. Moch, and M. Zaro, Higgs Boson Production via Vector-Boson Fusion at Next-to-Next-to-Leading Order in QCD, Phys. Rev. Lett. **105,** 011801 (2010).

[17] P. Bolzoni, F. Maltoni, S.-O. Moch, and M. Zaro, Vector boson fusion at next-to-next-to-leading order in QCD: Standard model Higgs boson and beyond, Phys. Rev. D **85,** 035002 (2012).

[18] M. Cacciari, F. A. Dreyer, A. Karlberg, G. P. Salam, and G. Zanderighi, Fully Differential Vector-Boson-Fusion Higgs Production at Next-to-Next-to-Leading Order, Phys. Rev. Lett. **115,** 082002 (2015).Erratum, Phys. Rev. Lett. **120,** 139901 (2018).

[19] A. Denner, S. Dittmaier, S. Kallweit, and A. Mück, HAWK 2.0: A Monte Carlo program for Higgs production in vector-boson fusion and Higgs strahlung at hadron colliders, Comput. Phys. Commun. **195,** 161 (2015).

[20] ATLAS Collaboration, Search for the Standard Model Higgs boson produced by vector-boson fusion and decaying to bottom quarks in $\sqrt{s} = 8$ TeV pp collisions with the ATLAS detector, J. High Energy Phys. 11 (2016) 112.

[21] CMS Collaboration, Search for the standard model Higgs boson produced through vector boson fusion and decaying to $b\bar{b}$, Phys. Rev. D **92,** 032008 (2015).

[22] E. Gabrielli, F. Maltoni, B. Mele, M. Moretti, F. Piccinini, and R. Pittau, Higgs boson production in association with a photon in vector boson fusion at the LHC, Nucl. Phys. **B781,** 64 (2007).

[23] E. Gabrielli, B. Mele, F. Piccinini, and R. Pittau, Asking for an extra photon in Higgs production at the LHC and beyond, J. High Energy Phys. 07 (2016) 003.

[24] ATLAS Collaboration, The ATLAS Experiment at the CERN Large Hadron Collider, J. Instrum. **3,** S08003 (2008).

[25] ATLAS Collaboration, ATLAS insertable B-layer technical design report, Report No. CERN-LHCC-2010-013, 2010, http://cds.cern.ch/record/1291633.

[26] P. Nason, A new method for combining NLO QCD with shower Monte Carlo algorithms, J. High Energy Phys. 11 (2004) 040.

[27] S. Frixione, P. Nason, and C. Oleari, Matching NLO QCD computations with parton shower simulations: the POWHEG method, J. High Energy Phys. 11 (2007) 070.

[28] S. Alioli, P. Nason, C. Oleari, and E. Re, A general framework for implementing NLO calculations in shower Monte Carlo programs: The POWHEG BOX, J. High Energy Phys. 06 (2010) 043.

[29] H.-L. Lai, M. Guzzi, J. Huston, Z. Li, P. M. Nadolsky, J. Pumplin, and C.-P. Yuan, New parton distributions for collider physics, Phys. Rev. D **82,** 074024 (2010).

[30] T. Sjöstrand, S. Ask, J. R. Christiansen, R. Corke, N. Desai, P. Ilten, S. Mrenna, S. Prestel, C. O. Rasmussen, and P. Z. Skands, An introduction to PYTHIA 8.2, Comput. Phys. Commun. **191,** 159 (2015).

[31] ATLAS Collaboration, Measurement of the Z/γ^* boson transverse momentum distribution in pp collisions at $\sqrt{s} = 7$ TeV with the ATLAS detector, J. High Energy Phys. 09 (2014) 145.

[32] R. D. Ball et al., Parton distributions with LHC data, Nucl. Phys. **B867,** 244 (2013).

[33] J. Alwall, R. Frederix, S. Frixione, V. Hirschi, F. Maltoni, O. Mattelaer, H.-S. Shao, T. Stelzer, P. Torrielli, and M. Zaro, The automated computation of tree-level and next-to-leading order differential cross sections, and their matching to parton shower simulations, J. High Energy Phys. 07 (2014) 079.

[34] M. Bahr et al., Herwig++ physics and manual, Eur. Phys. J. C **58,** 639 (2008).

[35] ATLAS Collaboration, ATLAS Pythia 8 tunes to 7 TeV data, Report No. ATL-PHYS-PUB-2014-021, 2014, https://cds.cern.ch/record/1966419.

[36] J. Butterworth et al., PDF4LHC recommendations for LHC Run II, J. Phys. G **43,** 023001 (2016).

[37] T. Sjöstrand, S. Mrenna, and P. Z. Skands, A brief introduction to PYTHIA 8.1, Comput. Phys. Commun. **178,** 852 (2008).

[38] ATLAS Collaboration, Summary of ATLAS Pythia 8 tunes, Report No. ATL-PHYS-PUB-2012-003, 2012, https://cds.cern.ch/record/1474107.

[39] A. D. Martin, W. J. Stirling, R. S. Thorne, and G. Watt, Parton distributions for the LHC, Eur. Phys. J. C **63,** 189 (2009).

[40] ATLAS Collaboration, The ATLAS simulation infrastructure, Eur. Phys. J. C **70,** 823 (2010).

[41] S. Agostinelli et al., GEANT4—a simulation toolkit, Nucl. Instrum. Methods Phys. Res., Sect. A **506,** 250 (2003).

[42] ATLAS Collaboration, The simulation principle and performance of the ATLAS fast calorimeter simulation FastCaloSim, Report No. ATL-PHYS-PUB-2010-013, 2010, https://cds.cern.ch/record/1300517.

[43] M. Cacciari, G. P. Salam, and G. Soyez, The anti-k_t jet clustering algorithm, J. High Energy Phys. 04 (2008) 063.

[44] ATLAS Collaboration, Tagging and suppression of pileup jets with the ATLAS detector, Report No. ATLAS-CONF-2014-018, 2014, https://cds.cern.ch/record/1700870.

[45] ATLAS Collaboration, Jet energy scale measurements and their systematic uncertainties in proton–proton collisions at $\sqrt{s} = 13$ TeV with the ATLAS detector, Phys. Rev. D **96,** 072002 (2017).

[46] ATLAS Collaboration, Performance of *b*-jet identification in the ATLAS experiment, J. Instrum. **11**, P04008 (2016).

[47] ATLAS Collaboration, Optimisation of the ATLAS *b*-tagging performance for the 2016 LHC Run, Report No. ATL-PHYS-PUB-2016-012, 2016, https://cds.cern.ch/record/2160731.

[48] ATLAS Collaboration, Measurements of *b*-jet tagging efficiency with the ATLAS detector using $t\bar{t}$ events at $\sqrt{s} = 13$ TeV, arXiv:1805.01845.

[49] ATLAS Collaboration, Measurement of the photon identification efficiencies with the ATLAS detector using LHC Run-1 data, Eur. Phys. J. C **76**, 666 (2016).

[50] ATLAS Collaboration, Topological cell clustering in the ATLAS calorimeters and its performance in LHC Run 1, Eur. Phys. J. C **77**, 490 (2017).

[51] ATLAS Collaboration, Electron efficiency measurements with the ATLAS detector using the 2015 LHC proton-proton collision data, Repor No. ATLAS-CONF-2016-024, 2016, https://cds.cern.ch/record/2157687.

[52] ATLAS Collaboration, Electron efficiency measurements with the ATLAS detector using 2012 LHC proton-proton collision data, Eur. Phys. J. C **77**, 195 (2017).

[53] ATLAS Collaboration, Muon reconstruction performance of the ATLAS detector in proton–proton collision data at $\sqrt{s} = 13$ TeV, Eur. Phys. J. C **76**, 292 (2016).

[54] ATLAS Collaboration, Performance of the ATLAS trigger system in 2015, Eur. Phys. J. C **77**, 317 (2017).

[55] F. Pedregosa *et al.*, Scikit-learn: Machine learning in Python, J. Machine Learning Research **12**, 2825 (2011).

[56] A. Hoecker *et al.*, TMVA: Toolkit for multivariate data analysis, Proc. Sci., ACAT2007 (**2007**) 040 [arXiv:physics/0703039].

[57] Y. Freund and R. E. Schapire, A decision-theoretic generalization of on-line learning and an application to boosting, J. Comput. Syst. Sci. **55**, 119 (1997).

[58] A. D. Bukin, Fitting function for asymmetric peaks, arXiv:0711.4449.

[59] M. Oreglia, A study of the reactions $\psi' \to \gamma\gamma\psi$, Ph.D. thesis, Stanford University, 1980, https://www.slac.stanford.edu/cgi-wrap/getdoc/slac-r-236.pdf.

[60] T. Skwarnicki, *A Study of the Radiative Cascade Transitions Between the Upsilon-Prime and Upsilon Resonances* (INP, Cracow, 1986), https://inspirehep.net/record/230779/files/f31-86-02.pdf.

[61] G. Cowan, K. Cranmer, E. Gross, and O. Vitells, Asymptotic formulae for likelihood-based tests of new physics, Eur. Phys. J. C **71**, 1554 (2011); Erratum, Eur. Phys. J. C **73**, 2501 (2013).

[62] M. Rubin, G. P. Salam, and S. Sapeta, Giant QCD K-factors beyond NLO, J. High Energy Phys. 09 (2010) 084.

[63] ATLAS Collaboration, Luminosity determination in pp collisions at $\sqrt{s} = 8$ TeV using the ATLAS detector at the LHC, Eur. Phys. J. C **76**, 653 (2016).

[64] ATLAS Collaboration, Performance of the ATLAS track reconstruction algorithms in dense environments in LHC Run 2, Eur. Phys. J. C **77**, 673 (2017).

[65] ATLAS Collaboration, Measurement of the charged-particle multiplicity inside jets from $\sqrt{s} = 8$ TeV pp collisions with the ATLAS detector, Eur. Phys. J. C **76**, 322 (2016).

[66] ATLAS Collaboration, Electron and photon energy calibration with the ATLAS detector using data collected in 2015 at $\sqrt{s} = 13$ TeV, Report No. ATL-PHYS-PUB-2016-015, 2016, https://cds.cern.ch/record/2203514.

[67] ATLAS Collaboration, Photon identification in 2015 ATLAS data, Report No. ATL-PHYS-PUB-2016-014, 2016, https://cds.cern.ch/record/2203125.

[68] D. de Florian *et al.*, Handbook of LHC Higgs cross sections: 4. Deciphering the nature of the Higgs sector, CERN Report No. CERN-2017-002-M, 2017, http://dx.doi.org/10.23731/CYRM-2017-002.

[69] A. L. Read, Presentation of search results: The CLs technique, J. Phys. G **28**, 2693 (2002).

[70] ATLAS Collaboration, ATLAS computing acknowledgements, Report No. ATL-GEN-PUB-2016-002, https://cds.cern.ch/record/2202407.

M. Aaboud,[34d] G. Aad,[99] B. Abbott,[124] O. Abdinov,[13,a] B. Abeloos,[128] D. K. Abhayasinghe,[91] S. H. Abidi,[164] O. S. AbouZeid,[39] N. L. Abraham,[153] H. Abramowicz,[158] H. Abreu,[157] Y. Abulaiti,[6] B. S. Acharya,[64a,64b,b] S. Adachi,[160] L. Adamczyk,[81a] J. Adelman,[119] M. Adersberger,[112] A. Adiguzel,[12c,c] T. Adye,[141] A. A. Affolder,[143] Y. Afik,[157] C. Agheorghiesei,[27c] J. A. Aguilar-Saavedra,[136f,136a] F. Ahmadov,[77,d] G. Aielli,[71a,71b] S. Akatsuka,[83] T. P. A. Åkesson,[94] E. Akilli,[52] A. V. Akimov,[108] G. L. Alberghi,[23b,23a] J. Albert,[173] P. Albicocco,[49] M. J. Alconada Verzini,[86] S. Alderweireldt,[117] M. Aleksa,[35] I. N. Aleksandrov,[77] C. Alexa,[27b] T. Alexopoulos,[10] M. Alhroob,[124] B. Ali,[138] G. Alimonti,[66a] J. Alison,[36] S. P. Alkire,[145] C. Allaire,[128] B. M. M. Allbrooke,[153] B. W. Allen,[127] P. P. Allport,[21] A. Aloisio,[67a,67b] A. Alonso,[39] F. Alonso,[86] C. Alpigiani,[145] A. A. Alshehri,[55] M. I. Alstaty,[99] B. Alvarez Gonzalez,[35] D. Álvarez Piqueras,[171] M. G. Alviggi,[67a,67b] B. T. Amadio,[18] Y. Amaral Coutinho,[78b] L. Ambroz,[131] C. Amelung,[26] D. Amidei,[103] S. P. Amor Dos Santos,[136a,136c] S. Amoroso,[44] C. S. Amrouche,[52] C. Anastopoulos,[146] L. S. Ancu,[52] N. Andari,[21] T. Andeen,[11] C. F. Anders,[59b] J. K. Anders,[20] K. J. Anderson,[36] A. Andreazza,[66a,66b] V. Andrei,[59a] C. R. Anelli,[173] S. Angelidakis,[37] I. Angelozzi,[118] A. Angerami,[38] A. V. Anisenkov,[120b,120a] A. Annovi,[69a] C. Antel,[59a] M. T. Anthony,[146] M. Antonelli,[49] D. J. A. Antrim,[168] F. Anulli,[70a] M. Aoki,[79] J. A. Aparisi Pozo,[171] L. Aperio Bella,[35] G. Arabidze,[104] J. P. Araque,[136a] V. Araujo Ferraz,[78b] R. Araujo Pereira,[78b] A. T. H. Arce,[47] R. E. Ardell,[91] F. A. Arduh,[86] J-F. Arguin,[107] S. Argyropoulos,[75] A. J. Armbruster,[35] L. J. Armitage,[90] A Armstrong,[168] O. Arnaez,[164] H. Arnold,[118]

M. Arratia,[31] O. Arslan,[24] A. Artamonov,[109,a] G. Artoni,[131] S. Artz,[97] S. Asai,[160] N. Asbah,[44] A. Ashkenazi,[158] E. M. Asimakopoulou,[169] L. Asquith,[153] K. Assamagan,[29] R. Astalos,[28a] R. J. Atkin,[32a] M. Atkinson,[170] N. B. Atlay,[148] K. Augsten,[138] G. Avolio,[35] R. Avramidou,[58a] M. K. Ayoub,[15a] G. Azuelos,[107,e] A. E. Baas,[59a] M. J. Baca,[21] H. Bachacou,[142] K. Bachas,[65a,65b] M. Backes,[131] P. Bagnaia,[70a,70b] M. Bahmani,[82] H. Bahrasemani,[149] A. J. Bailey,[171] J. T. Baines,[141] M. Bajic,[39] C. Bakalis,[10] O. K. Baker,[180] P. J. Bakker,[118] D. Bakshi Gupta,[93] E. M. Baldin,[120b,120a] P. Balek,[177] F. Balli,[142] W. K. Balunas,[133] J. Balz,[97] E. Banas,[82] A. Bandyopadhyay,[24] S. Banerjee,[178,f] A. A. E. Bannoura,[179] L. Barak,[158] W. M. Barbe,[37] E. L. Barberio,[102] D. Barberis,[53b,53a] M. Barbero,[99] T. Barillari,[113] M-S. Barisits,[35] J. Barkeloo,[127] T. Barklow,[150] N. Barlow,[31] R. Barnea,[157] S. L. Barnes,[58c] B. M. Barnett,[141] R. M. Barnett,[18] Z. Barnovska-Blenessy,[58a] A. Baroncelli,[72a] G. Barone,[26] A. J. Barr,[131] L. Barranco Navarro,[171] F. Barreiro,[96] J. Barreiro Guimarães da Costa,[15a] R. Bartoldus,[150] A. E. Barton,[87] P. Bartos,[28a] A. Basalaev,[134] A. Bassalat,[128] R. L. Bates,[55] S. J. Batista,[164] S. Batlamous,[34e] J. R. Batley,[31] M. Battaglia,[143] M. Bauce,[70a,70b] F. Bauer,[142] K. T. Bauer,[168] H. S. Bawa,[150,g] J. B. Beacham,[122] M. D. Beattie,[87] T. Beau,[132] P. H. Beauchemin,[167] P. Bechtle,[24] H. C. Beck,[51] H. P. Beck,[20,h] K. Becker,[50] M. Becker,[97] C. Becot,[44] A. Beddall,[12d] A. J. Beddall,[12a] V. A. Bednyakov,[77] M. Bedognetti,[118] C. P. Bee,[152] T. A. Beermann,[35] M. Begalli,[78b] M. Begel,[29] A. Behera,[152] J. K. Behr,[44] A. S. Bell,[92] G. Bella,[158] L. Bellagamba,[23b] A. Bellerive,[33] M. Bellomo,[157] P. Bellos,[9] K. Belotskiy,[110] N. L. Belyaev,[110] O. Benary,[158,a] D. Benchekroun,[34a] M. Bender,[112] N. Benekos,[10] Y. Benhammou,[158] E. Benhar Noccioli,[180] J. Benitez,[75] D. P. Benjamin,[47] M. Benoit,[52] J. R. Bensinger,[26] S. Bentvelsen,[118] L. Beresford,[131] M. Beretta,[49] D. Berge,[44] E. Bergeaas Kuutmann,[169] N. Berger,[5] L. J. Bergsten,[26] J. Beringer,[18] S. Berlendis,[7] N. R. Bernard,[100] G. Bernardi,[132] C. Bernius,[150] F. U. Bernlochner,[24] T. Berry,[91] P. Berta,[97] C. Bertella,[15a] G. Bertoli,[43a,43b] I. A. Bertram,[87] G. J. Besjes,[39] O. Bessidskaia Bylund,[43a,43b] M. Bessner,[44] N. Besson,[142] A. Bethani,[98] S. Bethke,[113] A. Betti,[24] A. J. Bevan,[90] J. Beyer,[113] R. M. B. Bianchi,[135] O. Biebel,[112] D. Biedermann,[19] R. Bielski,[98] K. Bierwagen,[97] N. V. Biesuz,[69a,69b] M. Biglietti,[72a] T. R. V. Billoud,[107] M. Bindi,[51] A. Bingul,[12d] C. Bini,[70a,70b] S. Biondi,[23b,23a] M. Birman,[177] T. Bisanz,[51] J. P. Biswal,[158] C. Bittrich,[46] D. M. Bjergaard,[47] J. E. Black,[150] K. M. Black,[25] T. Blazek,[28a] I. Bloch,[44] C. Blocker,[26] A. Blue,[55] U. Blumenschein,[90] Dr. Blunier,[144a] G. J. Bobbink,[118] V. S. Bobrovnikov,[120b,120a] S. S. Bocchetta,[94] A. Bocci,[47] D. Boerner,[179] D. Bogavac,[112] A. G. Bogdanchikov,[120b,120a] C. Bohm,[43a] V. Boisvert,[91] P. Bokan,[169,i] T. Bold,[81a] A. S. Boldyrev,[111] A. E. Bolz,[59b] M. Bomben,[132] M. Bona,[90] J. S. Bonilla,[127] M. Boonekamp,[142] A. Borisov,[140] G. Borissov,[87] J. Bortfeldt,[35] D. Bortoletto,[131] V. Bortolotto,[71a,61b,61c,71b] D. Boscherini,[23b] M. Bosman,[14] J. D. Bossio Sola,[30] K. Bouaouda,[34a] J. Boudreau,[135] E. V. Bouhova-Thacker,[87] D. Boumediene,[37] C. Bourdarios,[128] S. K. Boutle,[55] A. Boveia,[122] J. Boyd,[35] I. R. Boyko,[77] A. J. Bozson,[91] J. Bracinik,[21] N. Brahimi,[99] A. Brandt,[8] G. Brandt,[179] O. Brandt,[59a] F. Braren,[44] U. Bratzler,[161] B. Brau,[100] J. E. Brau,[127] W. D. Breaden Madden,[55] K. Brendlinger,[44] A. J. Brennan,[102] L. Brenner,[44] R. Brenner,[169] S. Bressler,[177] B. Brickwedde,[97] D. L. Briglin,[21] D. Britton,[55] D. Britzger,[59b] I. Brock,[24] R. Brock,[104] G. Brooijmans,[38] T. Brooks,[91] W. K. Brooks,[144b] E. Brost,[119] J. H Broughton,[21] P. A. Bruckman de Renstrom,[82] D. Bruncko,[28b] A. Bruni,[23b] G. Bruni,[23b] L. S. Bruni,[118] S. Bruno,[71a,71b] B. H. Brunt,[31] M. Bruschi,[23b] N. Bruscino,[135] P. Bryant,[36] L. Bryngemark,[44] T. Buanes,[17] Q. Buat,[35] P. Buchholz,[148] A. G. Buckley,[55] I. A. Budagov,[77] F. Buehrer,[50] M. K. Bugge,[130] O. Bulekov,[110] D. Bullock,[8] T. J. Burch,[119] S. Burdin,[88] C. D. Burgard,[118] A. M. Burger,[5] B. Burghgrave,[119] K. Burka,[82] S. Burke,[141] I. Burmeister,[45] J. T. P. Burr,[131] D. Büscher,[50] V. Büscher,[97] E. Buschmann,[51] P. Bussey,[55] J. M. Butler,[25] C. M. Buttar,[55] J. M. Butterworth,[92] P. Butti,[35] W. Buttinger,[35] A. Buzatu,[155] A. R. Buzykaev,[120b,120a] G. Cabras,[23b,23a] S. Cabrera Urbán,[171] D. Caforio,[138] H. Cai,[170] V. M. M. Cairo,[2] O. Cakir,[4a] N. Calace,[52] P. Calafiura,[18] A. Calandri,[99] G. Calderini,[132] P. Calfayan,[63] G. Callea,[40b,40a] L. P. Caloba,[78b] S. Calvente Lopez,[96] D. Calvet,[37] S. Calvet,[37] T. P. Calvet,[152] M. Calvetti,[69a,69b] R. Camacho Toro,[132] S. Camarda,[35] P. Camarri,[71a,71b] D. Cameron,[130] R. Caminal Armadans,[100] C. Camincher,[35] S. Campana,[35] M. Campanelli,[92] A. Camplani,[39] A. Campoverde,[148] V. Canale,[67a,67b] M. Cano Bret,[58c] J. Cantero,[125] T. Cao,[158] Y. Cao,[170] M. D. M. Capeans Garrido,[35] I. Caprini,[27b] M. Caprini,[27b] M. Capua,[40b,40a] R. M. Carbone,[38] R. Cardarelli,[71a] F. C. Cardillo,[50] I. Carli,[139] T. Carli,[35] G. Carlino,[67a] B. T. Carlson,[135] L. Carminati,[66a,66b] R. M. D. Carney,[43a,43b] S. Caron,[117] E. Carquin,[144b] S. Carrá,[66a,66b] G. D. Carrillo-Montoya,[35] D. Casadei,[32b] M. P. Casado,[14,j] A. F. Casha,[164] M. Casolino,[14] D. W. Casper,[168] R. Castelijn,[118] F. L. Castillo,[171] V. Castillo Gimenez,[171] N. F. Castro,[136a,136e] A. Catinaccio,[35] J. R. Catmore,[130] A. Cattai,[35] J. Caudron,[24] V. Cavaliere,[29] E. Cavallaro,[14] D. Cavalli,[66a] M. Cavalli-Sforza,[14] V. Cavasinni,[69a,69b] E. Celebi,[12b] F. Ceradini,[72a,72b] L. Cerda Alberich,[171] A. S. Cerqueira,[78a] A. Cerri,[153] L. Cerrito,[71a,71b] F. Cerutti,[18] A. Cervelli,[23b,23a] S. A. Cetin,[12b] A. Chafaq,[34a] D Chakraborty,[119] S. K. Chan,[57] W. S. Chan,[118] Y. L. Chan,[61a] J. D. Chapman,[31] D. G. Charlton,[21] C. C. Chau,[33] C. A. Chavez Barajas,[153] S. Che,[122] A. Chegwidden,[104] S. Chekanov,[6]

S. V. Chekulaev,[165a] G. A. Chelkov,[77,k] M. A. Chelstowska,[35] C. Chen,[58a] C. H. Chen,[76] H. Chen,[29] J. Chen,[58a] J. Chen,[38] S. Chen,[133] S. J. Chen,[15c] X. Chen,[15b,l] Y. Chen,[80] Y-H. Chen,[44] H. C. Cheng,[103] H. J. Cheng,[15d] A. Cheplakov,[77] E. Cheremushkina,[140] R. Cherkaoui El Moursli,[34e] E. Cheu,[7] K. Cheung,[62] L. Chevalier,[142] V. Chiarella,[49] G. Chiarelli,[69a] G. Chiodini,[65a] A. S. Chisholm,[35] A. Chitan,[27b] I. Chiu,[160] Y. H. Chiu,[173] M. V. Chizhov,[77] K. Choi,[63] A. R. Chomont,[128] S. Chouridou,[159] Y. S. Chow,[118] V. Christodoulou,[92] M. C. Chu,[61a] J. Chudoba,[137] A. J. Chuinard,[101] J. J. Chwastowski,[82] L. Chytka,[126] D. Cinca,[45] V. Cindro,[89] I. A. Cioară,[24] A. Ciocio,[18] F. Cirotto,[67a,67b] Z. H. Citron,[177] M. Citterio,[66a] A. Clark,[52] M. R. Clark,[38] P. J. Clark,[48] C. Clement,[43a,43b] Y. Coadou,[99] M. Cobal,[64a,64c] A. Coccaro,[53b,53a] J. Cochran,[76] A. E. C. Coimbra,[177] L. Colasurdo,[117] B. Cole,[38] A. P. Colijn,[118] J. Collot,[56] P. Conde Muiño,[136a,136b] E. Coniavitis,[50] S. H. Connell,[32b] I. A. Connelly,[98] S. Constantinescu,[27b] F. Conventi,[67a,m] A. M. Cooper-Sarkar,[131] F. Cormier,[172] K. J. R. Cormier,[164] M. Corradi,[70a,70b] E. E. Corrigan,[94] F. Corriveau,[101,n] A. Cortes-Gonzalez,[35] M. J. Costa,[171] D. Costanzo,[146] G. Cottin,[31] G. Cowan,[91] B. E. Cox,[98] J. Crane,[98] K. Cranmer,[121] S. J. Crawley,[55] R. A. Creager,[133] G. Cree,[33] S. Crépé-Renaudin,[56] F. Crescioli,[132] M. Cristinziani,[24] V. Croft,[121] G. Crosetti,[40b,40a] A. Cueto,[96] T. Cuhadar Donszelmann,[146] A. R. Cukierman,[150] J. Cúth,[97] S. Czekierda,[82] P. Czodrowski,[35] M. J. Da Cunha Sargedas De Sousa,[58b,136b] C. Da Via,[98] W. Dabrowski,[81a] T. Dado,[28a,i] S. Dahbi,[34e] T. Dai,[103] F. Dallaire,[107] C. Dallapiccola,[100] M. Dam,[39] G. D'amen,[23b,23a] J. Damp,[97] J. R. Dandoy,[133] M. F. Daneri,[30] N. P. Dang,[178,f] N. D Dann,[98] M. Danninger,[172] V. Dao,[35] G. Darbo,[53b] S. Darmora,[8] O. Dartsi,[5] A. Dattagupta,[127] T. Daubney,[44] S. D'Auria,[55] W. Davey,[24] C. David,[44] T. Davidek,[139] D. R. Davis,[47] E. Dawe,[102] I. Dawson,[146] K. De,[8] R. De Asmundis,[67a] A. De Benedetti,[124] M. De Beurs,[118] S. De Castro,[23b,23a] S. De Cecco,[70a,70b] N. De Groot,[117] P. de Jong,[118] H. De la Torre,[104] F. De Lorenzi,[76] A. De Maria,[51,o] D. De Pedis,[70a] A. De Salvo,[70a] U. De Sanctis,[71a,71b] A. De Santo,[153] K. De Vasconcelos Corga,[99] J. B. De Vivie De Regie,[128] C. Debenedetti,[143] D. V. Dedovich,[77] N. Dehghanian,[3] M. Del Gaudio,[40b,40a] J. Del Peso,[96] Y. Delabat Diaz,[44] D. Delgove,[128] F. Deliot,[142] C. M. Delitzsch,[7] M. Della Pietra,[67a,67b] D. Della Volpe,[52] A. Dell'Acqua,[35] L. Dell'Asta,[25] M. Delmastro,[5] C. Delporte,[128] P. A. Delsart,[56] D. A. DeMarco,[164] S. Demers,[180] M. Demichev,[77] S. P. Denisov,[140] D. Denysiuk,[118] L. D'Eramo,[132] D. Derendarz,[82] J. E. Derkaoui,[34d] F. Derue,[132] P. Dervan,[88] K. Desch,[24] C. Deterre,[44] K. Dette,[164] M. R. Devesa,[30] P. O. Deviveiros,[35] A. Dewhurst,[141] S. Dhaliwal,[26] F. A. Di Bello,[52] A. Di Ciaccio,[71a,71b] L. Di Ciaccio,[5] W. K. Di Clemente,[133] C. Di Donato,[67a,67b] A. Di Girolamo,[35] B. Di Micco,[72a,72b] R. Di Nardo,[100] K. F. Di Petrillo,[57] A. Di Simone,[50] R. Di Sipio,[164] D. Di Valentino,[33] C. Diaconu,[99] M. Diamond,[164] F. A. Dias,[39] T. Dias Do Vale,[136a] M. A. Diaz,[144a] J. Dickinson,[18] E. B. Diehl,[103] J. Dietrich,[19] S. Díez Cornell,[44] A. Dimitrievska,[18] J. Dingfelder,[24] F. Dittus,[35] F. Djama,[99] T. Djobava,[156b] J. I. Djuvsland,[59a] M. A. B. Do Vale,[78c] M. Dobre,[27b] D. Dodsworth,[26] C. Doglioni,[94] J. Dolejsi,[139] Z. Dolezal,[139] M. Donadelli,[78d] J. Donini,[37] A. D'onofrio,[90] M. D'Onofrio,[88] J. Dopke,[141] A. Doria,[67a] M. T. Dova,[86] A. T. Doyle,[55] E. Drechsler,[51] E. Dreyer,[149] T. Dreyer,[51] Y. Du,[58b] J. Duarte-Campderros,[158] F. Dubinin,[108] M. Dubovsky,[28a] A. Dubreuil,[52] E. Duchovni,[177] G. Duckeck,[112] A. Ducourthial,[132] O. A. Ducu,[107,p] D. Duda,[113] A. Dudarev,[35] A. C. Dudder,[97] E. M. Duffield,[18] L. Duflot,[128] M. Dührssen,[35] C. Dülsen,[179] M. Dumancic,[177] A. E. Dumitriu,[27b,q] A. K. Duncan,[55] M. Dunford,[59a] A. Duperrin,[99] H. Duran Yildiz,[4a] M. Düren,[54] A. Durglishvili,[156b] D. Duschinger,[46] B. Dutta,[44] D. Duvnjak,[1] M. Dyndal,[44] S. Dysch,[98] B. S. Dziedzic,[82] C. Eckardt,[44] K. M. Ecker,[113] R. C. Edgar,[103] T. Eifert,[35] G. Eigen,[17] K. Einsweiler,[18] T. Ekelof,[169] M. El Kacimi,[34c] R. El Kosseifi,[99] V. Ellajosyula,[99] M. Ellert,[169] F. Ellinghaus,[179] A. A. Elliot,[90] N. Ellis,[35] J. Elmsheuser,[29] M. Elsing,[35] D. Emeliyanov,[141] Y. Enari,[160] J. S. Ennis,[175] M. B. Epland,[47] J. Erdmann,[45] A. Ereditato,[20] S. Errede,[170] M. Escalier,[128] C. Escobar,[171] O. Estrada Pastor,[171] A. I. Etienvre,[142] E. Etzion,[158] H. Evans,[63] A. Ezhilov,[134] M. Ezzi,[34e] F. Fabbri,[55] L. Fabbri,[23b,23a] V. Fabiani,[117] G. Facini,[92] R. M. Faisca Rodrigues Pereira,[136a] R. M. Fakhrutdinov,[140] S. Falciano,[70a] P. J. Falke,[5] S. Falke,[5] J. Faltova,[139] Y. Fang,[15a] M. Fanti,[66a,66b] A. Farbin,[8] A. Farilla,[72a] E. M. Farina,[68a,68b] T. Farooque,[104] S. Farrell,[18] S. M. Farrington,[175] P. Farthouat,[35] F. Fassi,[34e] P. Fassnacht,[35] D. Fassouliotis,[9] M. Faucci Giannelli,[48] A. Favareto,[53b,53a] W. J. Fawcett,[52] L. Fayard,[128] O. L. Fedin,[134,r] W. Fedorko,[172] M. Feickert,[41] S. Feigl,[130] L. Feligioni,[99] C. Feng,[58b] E. J. Feng,[35] M. Feng,[47] M. J. Fenton,[55] A. B. Fenyuk,[140] L. Feremenga,[8] J. Ferrando,[44] A. Ferrari,[169] P. Ferrari,[118] R. Ferrari,[68a] D. E. Ferreira de Lima,[59b] A. Ferrer,[171] D. Ferrere,[52] C. Ferretti,[103] F. Fiedler,[97] A. Filipčič,[89] F. Filthaut,[117] K. D. Finelli,[25] M. C. N. Fiolhais,[136a,136c,s] L. Fiorini,[171] C. Fischer,[14] W. C. Fisher,[104] N. Flaschel,[44] I. Fleck,[148] P. Fleischmann,[103] R. R. M. Fletcher,[133] T. Flick,[179] B. M. Flierl,[112] L. M. Flores,[133] L. R. Flores Castillo,[61a] N. Fomin,[17] G. T. Forcolin,[98] A. Formica,[142] F. A. Förster,[14] A. C. Forti,[98] A. G. Foster,[21] D. Fournier,[128] H. Fox,[87] S. Fracchia,[146] P. Francavilla,[69a,69b] M. Franchini,[23b,23a] S. Franchino,[59a] D. Francis,[35] L. Franconi,[130] M. Franklin,[57] M. Frate,[168] M. Fraternali,[68a,68b] D. Freeborn,[92] S. M. Fressard-Batraneanu,[35] B. Freund,[107] W. S. Freund,[78b] D. Froidevaux,[35]

J. A. Frost,[131] C. Fukunaga,[161] E. Fullana Torregrosa,[171] T. Fusayasu,[114] J. Fuster,[171] O. Gabizon,[157] A. Gabrielli,[23b,23a] A. Gabrielli,[18] G. P. Gach,[81a] S. Gadatsch,[52] P. Gadow,[113] G. Gagliardi,[53b,53a] L. G. Gagnon,[107] C. Galea,[27b] B. Galhardo,[136a,136c] E. J. Gallas,[131] B. J. Gallop,[141] P. Gallus,[138] G. Galster,[39] R. Gamboa Goni,[90] K. K. Gan,[122] S. Ganguly,[177] J. Gao,[58a] Y. Gao,[88] Y. S. Gao,[150,g] C. García,[171] J. E. García Navarro,[171] J. A. García Pascual,[15a] M. Garcia-Sciveres,[18] R. W. Gardner,[36] N. Garelli,[150] V. Garonne,[130] K. Gasnikova,[44] A. Gaudiello,[53b,53a] G. Gaudio,[68a] I. L. Gavrilenko,[108] A. Gavriljuk,[109] C. Gay,[172] G. Gaycken,[24] E. N. Gazis,[10] C. N. P. Gee,[141] J. Geisen,[51] M. Geisen,[97] M. P. Geisler,[59a] K. Gellerstedt,[43a,43b] C. Gemme,[53b] M. H. Genest,[56] C. Geng,[103] S. Gentile,[70a,70b] S. George,[91] D. Gerbaudo,[14] G. Gessner,[45] S. Ghasemi,[148] M. Ghasemi Bostanabad,[173] M. Ghneimat,[24] B. Giacobbe,[23b] S. Giagu,[70a,70b] N. Giangiacomi,[23b,23a] P. Giannetti,[69a] A. Giannini,[67a,67b] S. M. Gibson,[91] M. Gignac,[143] D. Gillberg,[33] G. Gilles,[179] D. M. Gingrich,[3,e] M. P. Giordani,[64a,64c] F. M. Giorgi,[23b] P. F. Giraud,[142] P. Giromini,[57] G. Giugliarelli,[64a,64c] D. Giugni,[66a] F. Giuli,[131] M. Giulini,[59b] S. Gkaitatzis,[159] I. Gkialas,[9,t] E. L. Gkougkousis,[14] P. Gkountoumis,[10] L. K. Gladilin,[111] C. Glasman,[96] J. Glatzer,[14] P. C. F. Glaysher,[44] A. Glazov,[44] M. Goblirsch-Kolb,[26] J. Godlewski,[82] S. Goldfarb,[102] T. Golling,[52] D. Golubkov,[140] A. Gomes,[136a,136b,136d] R. Goncalves Gama,[78a] R. Gonçalo,[136a] G. Gonella,[50] L. Gonella,[21] A. Gongadze,[77] F. Gonnella,[21] J. L. Gonski,[57] S. González de la Hoz,[171] S. Gonzalez-Sevilla,[52] L. Goossens,[35] P. A. Gorbounov,[109] H. A. Gordon,[29] B. Gorini,[35] E. Gorini,[65a,65b] A. Gorišek,[89] A. T. Goshaw,[47] C. Gössling,[45] M. I. Gostkin,[77] C. A. Gottardo,[24] C. R. Goudet,[128] D. Goujdami,[34c] A. G. Goussiou,[145] N. Govender,[32b,u] C. Goy,[5] E. Gozani,[157] I. Grabowska-Bold,[81a] P. O. J. Gradin,[169] E. C. Graham,[88] J. Gramling,[168] E. Gramstad,[130] S. Grancagnolo,[19] V. Gratchev,[134] P. M. Gravila,[27f] F. G. Gravili,[65a,65b] C. Gray,[55] H. M. Gray,[18] Z. D. Greenwood,[93,v] C. Grefe,[24] K. Gregersen,[92] I. M. Gregor,[44] P. Grenier,[150] K. Grevtsov,[44] J. Griffiths,[8] A. A. Grillo,[143] K. Grimm,[150] S. Grinstein,[14,w] Ph. Gris,[37] J.-F. Grivaz,[128] S. Groh,[97] E. Gross,[177] J. Grosse-Knetter,[51] G. C. Grossi,[93] Z. J. Grout,[92] C. Grud,[103] A. Grummer,[116] L. Guan,[103] W. Guan,[178] J. Guenther,[35] A. Guerguichon,[128] F. Guescini,[165a] D. Guest,[168] R. Gugel,[50] B. Gui,[122] T. Guillemin,[5] S. Guindon,[35] U. Gul,[55] C. Gumpert,[35] J. Guo,[58c] W. Guo,[103] Y. Guo,[58a,x] Z. Guo,[99] R. Gupta,[41] S. Gurbuz,[12c] G. Gustavino,[124] B. J. Gutelman,[157] P. Gutierrez,[124] C. Gutschow,[92] C. Guyot,[142] M. P. Guzik,[81a] C. Gwenlan,[131] C. B. Gwilliam,[88] A. Haas,[121] C. Haber,[18] H. K. Hadavand,[8] N. Haddad,[34e] A. Hadef,[58a] S. Hageböck,[24] M. Hagihara,[166] H. Hakobyan,[181,a] M. Haleem,[174] J. Haley,[125] G. Halladjian,[104] G. D. Hallewell,[99] K. Hamacher,[179] P. Hamal,[126] K. Hamano,[173] A. Hamilton,[32a] G. N. Hamity,[146] K. Han,[58a,y] L. Han,[58a] S. Han,[15d] K. Hanagaki,[79,z] M. Hance,[143] D. M. Handl,[112] B. Haney,[133] R. Hankache,[132] P. Hanke,[59a] E. Hansen,[94] J. B. Hansen,[39] J. D. Hansen,[39] M. C. Hansen,[24] P. H. Hansen,[39] K. Hara,[166] A. S. Hard,[178] T. Harenberg,[179] S. Harkusha,[105] P. F. Harrison,[175] N. M. Hartmann,[112] Y. Hasegawa,[147] A. Hasib,[48] S. Hassani,[142] S. Haug,[20] R. Hauser,[104] L. Hauswald,[46] L. B. Havener,[38] M. Havranek,[138] C. M. Hawkes,[21] R. J. Hawkings,[35] D. Hayden,[104] C. Hayes,[152] C. P. Hays,[131] J. M. Hays,[90] H. S. Hayward,[88] S. J. Haywood,[141] M. P. Heath,[48] V. Hedberg,[94] L. Heelan,[8] S. Heer,[24] K. K. Heidegger,[50] J. Heilman,[33] S. Heim,[44] T. Heim,[18] B. Heinemann,[44,aa] J. J. Heinrich,[112] L. Heinrich,[121] C. Heinz,[54] J. Hejbal,[137] L. Helary,[35] A. Held,[172] S. Hellesund,[130] S. Hellman,[43a,43b] C. Helsens,[35] R. C. W. Henderson,[87] Y. Heng,[178] S. Henkelmann,[172] A. M. Henriques Correia,[35] G. H. Herbert,[19] H. Herde,[26] V. Herget,[174] Y. Hernández Jiménez,[32c] H. Herr,[97] M. G. Herrmann,[112] G. Herten,[50] R. Hertenberger,[112] L. Hervas,[35] T. C. Herwig,[133] G. G. Hesketh,[92] N. P. Hessey,[165a] J. W. Hetherly,[41] S. Higashino,[79] E. Higón-Rodriguez,[171] K. Hildebrand,[36] E. Hill,[173] J. C. Hill,[31] K. K. Hill,[29] K. H. Hiller,[44] S. J. Hillier,[21] M. Hils,[46] I. Hinchliffe,[18] M. Hirose,[129] D. Hirschbuehl,[179] B. Hiti,[89] O. Hladik,[137] D. R. Hlaluku,[32c] X. Hoad,[48] J. Hobbs,[152] N. Hod,[165a] M. C. Hodgkinson,[146] A. Hoecker,[35] M. R. Hoeferkamp,[116] F. Hoenig,[112] D. Hohn,[24] D. Hohov,[128] T. R. Holmes,[36] M. Holzbock,[112] M. Homann,[45] S. Honda,[166] T. Honda,[79] T. M. Hong,[135] A. Hönle,[113] B. H. Hooberman,[170] W. H. Hopkins,[127] Y. Horii,[115] P. Horn,[46] A. J. Horton,[149] L. A. Horyn,[36] J-Y. Hostachy,[56] A. Hostiuc,[145] S. Hou,[155] A. Hoummada,[34a] J. Howarth,[98] J. Hoya,[86] M. Hrabovsky,[126] J. Hrdinka,[35] I. Hristova,[19] J. Hrivnac,[128] A. Hrynevich,[106] T. Hryn'ova,[5] P. J. Hsu,[62] S.-C. Hsu,[145] Q. Hu,[29] S. Hu,[58c] Y. Huang,[15a] Z. Hubacek,[138] F. Hubaut,[99] M. Huebner,[24] F. Huegging,[24] T. B. Huffman,[131] E. W. Hughes,[38] M. Huhtinen,[35] R. F. H. Hunter,[33] P. Huo,[152] A. M. Hupe,[33] N. Huseynov,[77,d] J. Huston,[104] J. Huth,[57] R. Hyneman,[103] G. Iacobucci,[52] G. Iakovidis,[29] I. Ibragimov,[148] L. Iconomidou-Fayard,[128] Z. Idrissi,[34e] P. Iengo,[35] R. Ignazzi,[39] O. Igonkina,[118,bb] R. Iguchi,[160] T. Iizawa,[52] Y. Ikegami,[79] M. Ikeno,[79] D. Iliadis,[159] N. Ilic,[150] F. Iltzsche,[46] G. Introzzi,[68a,68b] M. Iodice,[72a] K. Iordanidou,[38] V. Ippolito,[70a,70b] M. F. Isacson,[169] N. Ishijima,[129] M. Ishino,[160] M. Ishitsuka,[162] W. Islam,[125] C. Issever,[131] S. Istin,[12c,cc] F. Ito,[166] J. M. Iturbe Ponce,[61a] R. Iuppa,[73a,73b] A. Ivina,[177] H. Iwasaki,[79] J. M. Izen,[42] V. Izzo,[67a] P. Jacka,[137] P. Jackson,[1] R. M. Jacobs,[24] V. Jain,[2] G. Jäkel,[179] K. B. Jakobi,[97] K. Jakobs,[50] S. Jakobsen,[74] T. Jakoubek,[137] D. O. Jamin,[125]

D. K. Jana,[93] R. Jansky,[52] J. Janssen,[24] M. Janus,[51] P. A. Janus,[81a] G. Jarlskog,[94] N. Javadov,[77,d] T. Javůrek,[50] M. Javurkova,[50] F. Jeanneau,[142] L. Jeanty,[18] J. Jejelava,[156a,dd] A. Jelinskas,[175] P. Jenni,[50,ee] J. Jeong,[44] S. Jézéquel,[5] H. Ji,[178] J. Jia,[152] H. Jiang,[76] Y. Jiang,[58a] Z. Jiang,[150,ff] S. Jiggins,[50] F. A. Jimenez Morales,[37] J. Jimenez Pena,[171] S. Jin,[15c] A. Jinaru,[27b] O. Jinnouchi,[162] H. Jivan,[32c] P. Johansson,[146] K. A. Johns,[7] C. A. Johnson,[63] W. J. Johnson,[145] K. Jon-And,[43a,43b] R. W. L. Jones,[87] S. D. Jones,[153] S. Jones,[7] T. J. Jones,[88] J. Jongmanns,[59a] P. M. Jorge,[136a,136b] J. Jovicevic,[165a] X. Ju,[178] J. J. Junggeburth,[113] A. Juste Rozas,[14,w] A. Kaczmarska,[82] M. Kado,[128] H. Kagan,[122] M. Kagan,[150] T. Kaji,[176] E. Kajomovitz,[157] C. W. Kalderon,[94] A. Kaluza,[97] S. Kama,[41] A. Kamenshchikov,[140] L. Kanjir,[89] Y. Kano,[160] V. A. Kantserov,[110] J. Kanzaki,[79] B. Kaplan,[121] L. S. Kaplan,[178] D. Kar,[32c] M. J. Kareem,[165b] E. Karentzos,[10] S. N. Karpov,[77] Z. M. Karpova,[77] V. Kartvelishvili,[87] A. N. Karyukhin,[140] K. Kasahara,[166] L. Kashif,[178] R. D. Kass,[122] A. Kastanas,[151] Y. Kataoka,[160] C. Kato,[160] J. Katzy,[44] K. Kawade,[80] K. Kawagoe,[85] T. Kawamoto,[160] G. Kawamura,[51] E. F. Kay,[88] V. F. Kazanin,[120b,120a] R. Keeler,[173] R. Kehoe,[41] J. S. Keller,[33] E. Kellermann,[94] J. J. Kempster,[21] J. Kendrick,[21] O. Kepka,[137] S. Kersten,[179] B. P. Kerševan,[89] R. A. Keyes,[101] M. Khader,[170] F. Khalil-Zada,[13] A. Khanov,[125] A. G. Kharlamov,[120b,120a] T. Kharlamova,[120b,120a] A. Khodinov,[163] T. J. Khoo,[52] E. Khramov,[77] J. Khubua,[156b] S. Kido,[80] M. Kiehn,[52] C. R. Kilby,[91] S. H. Kim,[166] Y. K. Kim,[36] N. Kimura,[64a,64c] O. M. Kind,[19] B. T. King,[88] D. Kirchmeier,[46] J. Kirk,[141] A. E. Kiryunin,[113] T. Kishimoto,[160] D. Kisielewska,[81a] V. Kitali,[44] O. Kivernyk,[5] E. Kladiva,[28b] T. Klapdor-Kleingrothaus,[50] M. H. Klein,[103] M. Klein,[88] U. Klein,[88] K. Kleinknecht,[97] P. Klimek,[119] A. Klimentov,[29] R. Klingenberg,[45,a] T. Klingl,[24] T. Klioutchnikova,[35] F. F. Klitzner,[112] P. Kluit,[118] S. Kluth,[113] E. Kneringer,[74] E. B. F. G. Knoops,[99] A. Knue,[50] A. Kobayashi,[160] D. Kobayashi,[85] T. Kobayashi,[160] M. Kobel,[46] M. Kocian,[150] P. Kodys,[139] T. Koffas,[33] E. Koffeman,[118] N. M. Köhler,[113] T. Koi,[150] M. Kolb,[59b] I. Koletsou,[5] T. Kondo,[79] N. Kondrashova,[58c] K. Köneke,[50] A. C. König,[117] T. Kono,[79] R. Konoplich,[121,gg] V. Konstantinides,[92] N. Konstantinidis,[92] B. Konya,[94] R. Kopeliansky,[63] S. Koperny,[81a] K. Korcyl,[82] K. Kordas,[159] A. Korn,[92] I. Korolkov,[14] E. V. Korolkova,[146] O. Kortner,[113] S. Kortner,[113] T. Kosek,[139] V. V. Kostyukhin,[24] A. Kotwal,[47] A. Koulouris,[10] A. Kourkoumeli-Charalampidi,[68a,68b] C. Kourkoumelis,[9] E. Kourlitis,[146] V. Kouskoura,[29] A. B. Kowalewska,[82] R. Kowalewski,[173] T. Z. Kowalski,[81a] C. Kozakai,[160] W. Kozanecki,[142] A. S. Kozhin,[140] V. A. Kramarenko,[111] G. Kramberger,[89] D. Krasnopevtsev,[110] M. W. Krasny,[132] A. Krasznahorkay,[35] D. Krauss,[113] J. A. Kremer,[81a] J. Kretzschmar,[88] P. Krieger,[164] K. Krizka,[18] K. Kroeninger,[45] H. Kroha,[113] J. Kroll,[137] J. Kroll,[133] J. Krstic,[16] U. Kruchonak,[77] H. Krüger,[24] N. Krumnack,[76] M. C. Kruse,[47] T. Kubota,[102] S. Kuday,[4b] J. T. Kuechler,[179] S. Kuehn,[35] A. Kugel,[59a] F. Kuger,[174] T. Kuhl,[44] V. Kukhtin,[77] R. Kukla,[99] Y. Kulchitsky,[105] S. Kuleshov,[144b] Y. P. Kulinich,[170] M. Kuna,[56] T. Kunigo,[83] A. Kupco,[137] T. Kupfer,[45] O. Kuprash,[158] H. Kurashige,[80] L. L. Kurchaninov,[165a] Y. A. Kurochkin,[105] M. G. Kurth,[15d] E. S. Kuwertz,[173] M. Kuze,[162] J. Kvita,[126] T. Kwan,[101] A. La Rosa,[113] J. L. La Rosa Navarro,[78d] L. La Rotonda,[40b,40a] F. La Ruffa,[40b,40a] C. Lacasta,[171] F. Lacava,[70a,70b] J. Lacey,[44] D. P. J. Lack,[98] H. Lacker,[19] D. Lacour,[132] E. Ladygin,[77] R. Lafaye,[5] B. Laforge,[132] T. Lagouri,[32c] S. Lai,[51] S. Lammers,[63] W. Lampl,[7] E. Lançon,[29] U. Landgraf,[50] M. P. J. Landon,[90] M. C. Lanfermann,[52] V. S. Lang,[44] J. C. Lange,[14] R. J. Langenberg,[35] A. J. Lankford,[168] F. Lanni,[29] K. Lantzsch,[24] A. Lanza,[68a] A. Lapertosa,[53b,53a] S. Laplace,[132] J. F. Laporte,[142] T. Lari,[66a] F. Lasagni Manghi,[23b,23a] M. Lassnig,[35] T. S. Lau,[61a] A. Laudrain,[128] M. Lavorgna,[67a,67b] A. T. Law,[143] P. Laycock,[88] M. Lazzaroni,[66a,66b] B. Le,[102] O. Le Dortz,[132] E. Le Guirriec,[99] E. P. Le Quilleuc,[142] M. LeBlanc,[7] T. LeCompte,[6] F. Ledroit-Guillon,[56] C. A. Lee,[29] G. R. Lee,[144a] L. Lee,[57] S. C. Lee,[155] B. Lefebvre,[101] M. Lefebvre,[173] F. Legger,[112] C. Leggett,[18] N. Lehmann,[179] G. Lehmann Miotto,[35] W. A. Leight,[44] A. Leisos,[159,hh] M. A. L. Leite,[78d] R. Leitner,[139] D. Lellouch,[177] B. Lemmer,[51] K. J. C. Leney,[92] T. Lenz,[24] B. Lenzi,[35] R. Leone,[7] S. Leone,[69a] C. Leonidopoulos,[48] G. Lerner,[153] C. Leroy,[107] R. Les,[164] A. A. J. Lesage,[142] C. G. Lester,[31] M. Levchenko,[134] J. Levêque,[5] D. Levin,[103] L. J. Levinson,[177] D. Lewis,[90] B. Li,[103] C-Q. Li,[58a] H. Li,[58b] L. Li,[58c] Q. Li,[15d] Q. Y. Li,[58a] S. Li,[58d,58c] X. Li,[58c] Y. Li,[148] Z. Liang,[15a] B. Liberti,[71a] A. Liblong,[164] K. Lie,[61c] S. Liem,[118] A. Limosani,[154] C. Y. Lin,[31] K. Lin,[104] T. H. Lin,[97] R. A. Linck,[63] B. E. Lindquist,[152] A. L. Lionti,[52] E. Lipeles,[133] A. Lipniacka,[17] M. Lisovyi,[59b] T. M. Liss,[170,ii] A. Lister,[172] A. M. Litke,[143] J. D. Little,[8] B. Liu,[76] B. L. Liu,[6] H. B. Liu,[29] H. Liu,[103] J. B. Liu,[58a] J. K. K. Liu,[131] K. Liu,[132] M. Liu,[58a] P. Liu,[18] Y. Liu,[15a] Y. L. Liu,[58a] Y. W. Liu,[58a] M. Livan,[68a,68b] A. Lleres,[56] J. Llorente Merino,[15a] S. L. Lloyd,[90] C. Y. Lo,[61b] F. Lo Sterzo,[41] E. M. Lobodzinska,[44] P. Loch,[7] A. Loesle,[50] K. M. Loew,[26] T. Lohse,[19] K. Lohwasser,[146] M. Lokajicek,[137] B. A. Long,[25] J. D. Long,[170] R. E. Long,[87] L. Longo,[65a,65b] K. A. Looper,[122] J. A. Lopez,[144b] I. Lopez Paz,[14] A. Lopez Solis,[146] J. Lorenz,[112] N. Lorenzo Martinez,[5] M. Losada,[22] P. J. Lösel,[112] X. Lou,[44] X. Lou,[15a] A. Lounis,[128] J. Love,[6] P. A. Love,[87] J. J. Lozano Bahilo,[171] H. Lu,[61a] M. Lu,[58a] N. Lu,[103] Y. J. Lu,[62] H. J. Lubatti,[145] C. Luci,[70a,70b] A. Lucotte,[56] C. Luedtke,[50] F. Luehring,[63] I. Luise,[132] W. Lukas,[74] L. Luminari,[70a] B. Lund-Jensen,[151] M. S. Lutz,[100]

P. M. Luzi,[132] D. Lynn,[29] R. Lysak,[137] E. Lytken,[94] F. Lyu,[15a] V. Lyubushkin,[77] H. Ma,[29] L. L. Ma,[58b] Y. Ma,[58b] G. Maccarrone,[49] A. Macchiolo,[113] C. M. Macdonald,[146] J. Machado Miguens,[133,136b] D. Madaffari,[171] R. Madar,[37] W. F. Mader,[46] A. Madsen,[44] N. Madysa,[46] J. Maeda,[80] K. Maekawa,[160] S. Maeland,[17] T. Maeno,[29] A. S. Maevskiy,[111] V. Magerl,[50] C. Maidantchik,[78b] T. Maier,[112] A. Maio,[136a,136b,136d] O. Majersky,[28a] S. Majewski,[127] Y. Makida,[79] N. Makovec,[128] B. Malaescu,[132] Pa. Malecki,[82] V. P. Maleev,[134] F. Malek,[56] U. Mallik,[75] D. Malon,[6] C. Malone,[31] S. Maltezos,[10] S. Malyukov,[35] J. Mamuzic,[171] G. Mancini,[49] I. Mandić,[89] J. Maneira,[136a] L. Manhaes de Andrade Filho,[78a] J. Manjarres Ramos,[46] K. H. Mankinen,[94] A. Mann,[112] A. Manousos,[74] B. Mansoulie,[142] J. D. Mansour,[15a] M. Mantoani,[51] S. Manzoni,[66a,66b] G. Marceca,[30] L. March,[52] L. Marchese,[131] G. Marchiori,[132] M. Marcisovsky,[137] C. A. Marin Tobon,[35] M. Marjanovic,[37] D. E. Marley,[103] F. Marroquim,[78b] Z. Marshall,[18] M. U. F Martensson,[169] S. Marti-Garcia,[171] C. B. Martin,[122] T. A. Martin,[175] V. J. Martin,[48] B. Martin dit Latour,[17] M. Martinez,[14,w] V. I. Martinez Outschoorn,[100] S. Martin-Haugh,[141] V. S. Martoiu,[27b] A. C. Martyniuk,[92] A. Marzin,[35] L. Masetti,[97] T. Mashimo,[160] R. Mashinistov,[108] J. Masik,[98] A. L. Maslennikov,[120b,120a] L. H. Mason,[102] L. Massa,[71a,71b] P. Massarotti,[67a,67b] P. Mastrandrea,[5] A. Mastroberardino,[40b,40a] T. Masubuchi,[160] P. Mättig,[179] J. Maurer,[27b] B. Maček,[89] S. J. Maxfield,[88] D. A. Maximov,[120b,120a] R. Mazini,[155] I. Maznas,[159] S. M. Mazza,[143] N. C. Mc Fadden,[116] G. Mc Goldrick,[164] S. P. Mc Kee,[103] A. McCarn,[103] T. G. McCarthy,[113] L. I. McClymont,[92] E. F. McDonald,[102] J. A. Mcfayden,[35] G. Mchedlidze,[51] M. A. McKay,[41] K. D. McLean,[173] S. J. McMahon,[141] P. C. McNamara,[102] C. J. McNicol,[175] R. A. McPherson,[173,n] J. E. Mdhluli,[32c] Z. A. Meadows,[100] S. Meehan,[145] T. M. Megy,[50] S. Mehlhase,[112] A. Mehta,[88] T. Meideck,[56] B. Meirose,[42] D. Melini,[171,jj] B. R. Mellado Garcia,[32c] J. D. Mellenthin,[51] M. Melo,[28a] F. Meloni,[44] A. Melzer,[24] S. B. Menary,[98] E. D. Mendes Gouveia,[136a] L. Meng,[88] X. T. Meng,[103] A. Mengarelli,[23b,23a] S. Menke,[113] E. Meoni,[40b,40a] S. Mergelmeyer,[19] C. Merlassino,[20] P. Mermod,[52] L. Merola,[67a,67b] C. Meroni,[66a] F. S. Merritt,[36] A. Messina,[70a,70b] J. Metcalfe,[6] A. S. Mete,[168] C. Meyer,[133] J. Meyer,[157] J-P. Meyer,[142] H. Meyer Zu Theenhausen,[59a] F. Miano,[153] R. P. Middleton,[141] L. Mijović,[48] G. Mikenberg,[177] M. Mikestikova,[137] M. Mikuž,[89] M. Milesi,[102] A. Milic,[164] D. A. Millar,[90] D. W. Miller,[36] A. Milov,[177] D. A. Milstead,[43a,43b] A. A. Minaenko,[140] M. Miñano Moya,[171] I. A. Minashvili,[156b] A. I. Mincer,[121] B. Mindur,[81a] M. Mineev,[77] Y. Minegishi,[160] Y. Ming,[178] L. M. Mir,[14] A. Mirto,[65a,65b] K. P. Mistry,[133] T. Mitani,[176] J. Mitrevski,[112] V. A. Mitsou,[171] A. Miucci,[20] P. S. Miyagawa,[146] A. Mizukami,[79] J. U. Mjörnmark,[94] T. Mkrtchyan,[181] M. Mlynarikova,[139] T. Moa,[43a,43b] K. Mochizuki,[107] P. Mogg,[50] S. Mohapatra,[38] S. Molander,[43a,43b] R. Moles-Valls,[24] M. C. Mondragon,[104] K. Mönig,[44] J. Monk,[39] E. Monnier,[99] A. Montalbano,[149] J. Montejo Berlingen,[35] F. Monticelli,[86] S. Monzani,[66a] R. W. Moore,[3] N. Morange,[128] D. Moreno,[22] M. Moreno Llácer,[35] P. Morettini,[53b] M. Morgenstern,[118] S. Morgenstern,[46] D. Mori,[149] T. Mori,[160] M. Morii,[57] M. Morinaga,[176] V. Morisbak,[130] A. K. Morley,[35] G. Mornacchi,[35] A. P. Morris,[92] J. D. Morris,[90] L. Morvaj,[152] P. Moschovakos,[10] M. Mosidze,[156b] H. J. Moss,[146] J. Moss,[150,kk] K. Motohashi,[162] R. Mount,[150] E. Mountricha,[35] E. J. W. Moyse,[100] S. Muanza,[99] F. Mueller,[113] J. Mueller,[135] R. S. P. Mueller,[112] D. Muenstermann,[87] P. Mullen,[55] G. A. Mullier,[20] F. J. Munoz Sanchez,[98] P. Murin,[28b] W. J. Murray,[175,141] A. Murrone,[66a,66b] M. Muškinja,[89] C. Mwewa,[32a] A. G. Myagkov,[140,ll] J. Myers,[127] M. Myska,[138] B. P. Nachman,[18] O. Nackenhorst,[45] K. Nagai,[131] K. Nagano,[79] Y. Nagasaka,[60] K. Nagata,[166] M. Nagel,[50] E. Nagy,[99] A. M. Nairz,[35] Y. Nakahama,[115] K. Nakamura,[79] T. Nakamura,[160] I. Nakano,[123] H. Nanjo,[129] F. Napolitano,[59a] R. F. Naranjo Garcia,[44] R. Narayan,[11] D. I. Narrias Villar,[59a] I. Naryshkin,[134] T. Naumann,[44] G. Navarro,[22] R. Nayyar,[7] H. A. Neal,[103] P. Y. Nechaeva,[108] T. J. Neep,[142] A. Negri,[68a,68b] M. Negrini,[23b] S. Nektarijevic,[117] C. Nellist,[51] M. E. Nelson,[131] S. Nemecek,[137] P. Nemethy,[121] M. Nessi,[35,mm] M. S. Neubauer,[170] M. Neumann,[179] P. R. Newman,[21] T. Y. Ng,[61c] Y. S. Ng,[19] H. D. N. Nguyen,[99] T. Nguyen Manh,[107] E. Nibigira,[37] R. B. Nickerson,[131] R. Nicolaidou,[142] J. Nielsen,[143] N. Nikiforou,[11] V. Nikolaenko,[140,ll] I. Nikolic-Audit,[132] K. Nikolopoulos,[21] P. Nilsson,[29] Y. Ninomiya,[79] A. Nisati,[70a] N. Nishu,[58c] R. Nisius,[113] I. Nitsche,[45] T. Nitta,[176] T. Nobe,[160] Y. Noguchi,[83] M. Nomachi,[129] I. Nomidis,[132] M. A. Nomura,[29] T. Nooney,[90] M. Nordberg,[35] N. Norjoharuddeen,[131] T. Novak,[89] O. Novgorodova,[46] R. Novotny,[138] L. Nozka,[126] K. Ntekas,[168] E. Nurse,[92] F. Nuti,[102] F. G. Oakham,[33,e] H. Oberlack,[113] T. Obermann,[24] J. Ocariz,[132] A. Ochi,[80] I. Ochoa,[38] J. P. Ochoa-Ricoux,[144a] K. O'Connor,[26] S. Oda,[85] S. Odaka,[79] S. Oerdek,[51] A. Oh,[98] S. H. Oh,[47] C. C. Ohm,[151] H. Oide,[53b,53a] H. Okawa,[166] Y. Okazaki,[83] Y. Okumura,[160] T. Okuyama,[79] A. Olariu,[27b] L. F. Oleiro Seabra,[136a] S. A. Olivares Pino,[144a] D. Oliveira Damazio,[29] J. L. Oliver,[1] M. J. R. Olsson,[36] A. Olszewski,[82] J. Olszowska,[82] D. C. O'Neil,[149] A. Onofre,[136a,136e] K. Onogi,[115] P. U. E. Onyisi,[11] H. Oppen,[130] M. J. Oreglia,[36] Y. Oren,[158] D. Orestano,[72a,72b] E. C. Orgill,[98] N. Orlando,[61b] A. A. O'Rourke,[44] R. S. Orr,[164] B. Osculati,[53b,53a,a] V. O'Shea,[55] R. Ospanov,[58a] G. Otero y Garzon,[30] H. Otono,[85] M. Ouchrif,[34d] F. Ould-Saada,[130] A. Ouraou,[142] Q. Ouyang,[15a] M. Owen,[55] R. E. Owen,[21] V. E. Ozcan,[12c] N. Ozturk,[8] J. Pacalt,[126] H. A. Pacey,[31] K. Pachal,[149]

A. Pacheco Pages,[14] L. Pacheco Rodriguez,[142] C. Padilla Aranda,[14] S. Pagan Griso,[18] M. Paganini,[180] G. Palacino,[63] S. Palazzo,[40b,40a] S. Palestini,[35] M. Palka,[81b] D. Pallin,[37] I. Panagoulias,[10] C. E. Pandini,[35] J. G. Panduro Vazquez,[91] P. Pani,[35] G. Panizzo,[64a,64c] L. Paolozzi,[52] T. D. Papadopoulou,[10] K. Papageorgiou,[9,t] A. Paramonov,[6] D. Paredes Hernandez,[61b] S. R. Paredes Saenz,[131] B. Parida,[58c] A. J. Parker,[87] K. A. Parker,[44] M. A. Parker,[31] F. Parodi,[53b,53a] J. A. Parsons,[38] U. Parzefall,[50] V. R. Pascuzzi,[164] J. M. P. Pasner,[143] E. Pasqualucci,[70a] S. Passaggio,[53b] F. Pastore,[91] P. Pasuwan,[43a,43b] S. Pataraia,[97] J. R. Pater,[98] A. Pathak,[178,f] T. Pauly,[35] B. Pearson,[113] M. Pedersen,[130] L. Pedraza Diaz,[117] R. Pedro,[136a,136b] S. V. Peleganchuk,[120b,120a] O. Penc,[137] C. Peng,[15d] H. Peng,[58a] B. S. Peralva,[78a] M. M. Perego,[142] A. P. Pereira Peixoto,[136a] D. V. Perepelitsa,[29] F. Peri,[19] L. Perini,[66a,66b] H. Pernegger,[35] S. Perrella,[67a,67b] V. D. Peshekhonov,[77,a] K. Peters,[44] R. F. Y. Peters,[98] B. A. Petersen,[35] T. C. Petersen,[39] E. Petit,[56] A. Petridis,[1] C. Petridou,[159] P. Petroff,[128] E. Petrolo,[70a] M. Petrov,[131] F. Petrucci,[72a,72b] M. Pettee,[180] N. E. Pettersson,[100] A. Peyaud,[142] R. Pezoa,[144b] T. Pham,[102] F. H. Phillips,[104] P. W. Phillips,[141] G. Piacquadio,[152] E. Pianori,[18] A. Picazio,[100] M. A. Pickering,[131] R. Piegaia,[30] J. E. Pilcher,[36] A. D. Pilkington,[98] M. Pinamonti,[71a,71b] J. L. Pinfold,[3] M. Pitt,[177] M-A. Pleier,[29] V. Pleskot,[139] E. Plotnikova,[77] D. Pluth,[76] P. Podberezko,[120b,120a] R. Poettgen,[94] R. Poggi,[52] L. Poggioli,[128] I. Pogrebnyak,[104] D. Pohl,[24] I. Pokharel,[51] G. Polesello,[68a] A. Poley,[44] A. Policicchio,[70a,70b] R. Polifka,[35] A. Polini,[23b] C. S. Pollard,[44] V. Polychronakos,[29] D. Ponomarenko,[110] L. Pontecorvo,[70a] G. A. Popeneciu,[27d] D. M. Portillo Quintero,[132] S. Pospisil,[138] K. Potamianos,[44] I. N. Potrap,[77] C. J. Potter,[31] H. Potti,[11] T. Poulsen,[94] J. Poveda,[35] T. D. Powell,[146] M. E. Pozo Astigarraga,[35] P. Pralavorio,[99] S. Prell,[76] D. Price,[98] M. Primavera,[65a] S. Prince,[101] N. Proklova,[110] K. Prokofiev,[61c] F. Prokoshin,[144b] S. Protopopescu,[29] J. Proudfoot,[6] M. Przybycien,[81a] A. Puri,[170] P. Puzo,[128] J. Qian,[103] Y. Qin,[98] A. Quadt,[51] M. Queitsch-Maitland,[44] A. Qureshi,[1] P. Rados,[102] F. Ragusa,[66a,66b] G. Rahal,[95] J. A. Raine,[98] S. Rajagopalan,[29] A. Ramirez Morales,[90] T. Rashid,[128] S. Raspopov,[5] M. G. Ratti,[66a,66b] D. M. Rauch,[44] F. Rauscher,[112] S. Rave,[97] B. Ravina,[146] I. Ravinovich,[177] J. H. Rawling,[98] M. Raymond,[35] A. L. Read,[130] N. P. Readioff,[56] M. Reale,[65a,65b] D. M. Rebuzzi,[68a,68b] A. Redelbach,[174] G. Redlinger,[29] R. Reece,[143] R. G. Reed,[32c] K. Reeves,[42] L. Rehnisch,[19] J. Reichert,[133] A. Reiss,[97] C. Rembser,[35] H. Ren,[15d] M. Rescigno,[70a] S. Resconi,[66a] E. D. Resseguie,[133] S. Rettie,[172] E. Reynolds,[21] O. L. Rezanova,[120b,120a] P. Reznicek,[139] E. Ricci,[73a,73b] R. Richter,[113] S. Richter,[92] E. Richter-Was,[81b] O. Ricken,[24] M. Ridel,[132] P. Rieck,[113] C. J. Riegel,[179] O. Rifki,[44] M. Rijssenbeek,[152] A. Rimoldi,[68a,68b] M. Rimoldi,[20] L. Rinaldi,[23b] G. Ripellino,[151] B. Ristić,[87] E. Ritsch,[35] I. Riu,[14] J. C. Rivera Vergara,[144a] F. Rizatdinova,[125] E. Rizvi,[90] C. Rizzi,[14] R. T. Roberts,[98] S. H. Robertson,[101,n] A. Robichaud-Veronneau,[101] D. Robinson,[31] J. E. M. Robinson,[44] A. Robson,[55] E. Rocco,[97] C. Roda,[69a,69b] Y. Rodina,[99] S. Rodriguez Bosca,[171] A. Rodriguez Perez,[14] D. Rodriguez Rodriguez,[171] A. M. Rodríguez Vera,[165b] S. Roe,[35] C. S. Rogan,[57] O. Røhne,[130] R. Röhrig,[113] C. P. A. Roland,[63] J. Roloff,[57] A. Romaniouk,[110] M. Romano,[23b,23a] N. Rompotis,[88] M. Ronzani,[121] L. Roos,[132] S. Rosati,[70a] K. Rosbach,[50] P. Rose,[143] N-A. Rosien,[51] E. Rossi,[44] E. Rossi,[67a,67b] L. P. Rossi,[53b] L. Rossini,[66a,66b] J. H. N. Rosten,[31] R. Rosten,[14] M. Rotaru,[27b] J. Rothberg,[145] D. Rousseau,[128] D. Roy,[32c] A. Rozanov,[99] Y. Rozen,[157] X. Ruan,[32c] F. Rubbo,[150] F. Rühr,[50] A. Ruiz-Martinez,[171] Z. Rurikova,[50] N. A. Rusakovich,[77] H. L. Russell,[101] J. P. Rutherfoord,[7] E. M. Rüttinger,[44,nn] Y. F. Ryabov,[134] M. Rybar,[170] G. Rybkin,[128] S. Ryu,[6] A. Ryzhov,[140] G. F. Rzehorz,[51] P. Sabatini,[51] G. Sabato,[118] S. Sacerdoti,[128] H. F-W. Sadrozinski,[143] R. Sadykov,[77] F. Safai Tehrani,[70a] P. Saha,[119] M. Sahinsoy,[59a] A. Sahu,[179] M. Saimpert,[44] M. Saito,[160] T. Saito,[160] H. Sakamoto,[160] A. Sakharov,[121,gg] D. Salamani,[52] G. Salamanna,[72a,72b] J. E. Salazar Loyola,[144b] D. Salek,[118] P. H. Sales De Bruin,[169] D. Salihagic,[113] A. Salnikov,[150] J. Salt,[171] D. Salvatore,[40b,40a] F. Salvatore,[153] A. Salvucci,[61a,61b,61c] A. Salzburger,[35] J. Samarati,[35] D. Sammel,[50] D. Sampsonidis,[159] D. Sampsonidou,[159] J. Sánchez,[171] A. Sanchez Pineda,[64a,64c] H. Sandaker,[130] C. O. Sander,[44] M. Sandhoff,[179] C. Sandoval,[22] D. P. C. Sankey,[141] M. Sannino,[53b,53a] Y. Sano,[115] A. Sansoni,[49] C. Santoni,[37] H. Santos,[136a] I. Santoyo Castillo,[153] A. Sapronov,[77] J. G. Saraiva,[136a,136d] O. Sasaki,[79] K. Sato,[166] E. Sauvan,[5] P. Savard,[164,e] N. Savic,[113] R. Sawada,[160] C. Sawyer,[141] L. Sawyer,[93,v] C. Sbarra,[23b] A. Sbrizzi,[23b,23a] T. Scanlon,[92] J. Schaarschmidt,[145] P. Schacht,[113] B. M. Schachtner,[112] D. Schaefer,[36] L. Schaefer,[133] J. Schaeffer,[97] S. Schaepe,[35] U. Schäfer,[97] A. C. Schaffer,[128] D. Schaile,[112] R. D. Schamberger,[152] N. Scharmberg,[98] V. A. Schegelsky,[134] D. Scheirich,[139] F. Schenck,[19] M. Schernau,[168] C. Schiavi,[53b,53a] S. Schier,[143] L. K. Schildgen,[24] Z. M. Schillaci,[26] E. J. Schioppa,[35] M. Schioppa,[40b,40a] K. E. Schleicher,[50] S. Schlenker,[35] K. R. Schmidt-Sommerfeld,[113] K. Schmieden,[35] C. Schmitt,[97] S. Schmitt,[44] S. Schmitz,[97] U. Schnoor,[50] L. Schoeffel,[142] A. Schoening,[59b] E. Schopf,[24] M. Schott,[97] J. F. P. Schouwenberg,[117] J. Schovancova,[35] S. Schramm,[52] A. Schulte,[97] H-C. Schultz-Coulon,[59a] M. Schumacher,[50] B. A. Schumm,[143] Ph. Schune,[142] A. Schwartzman,[150] T. A. Schwarz,[103] H. Schweiger,[98] Ph. Schwemling,[142] R. Schwienhorst,[104] A. Sciandra,[24] G. Sciolla,[26] M. Scornajenghi,[40b,40a] F. Scuri,[69a] F. Scutti,[102] L. M. Scyboz,[113] J. Searcy,[103] C. D. Sebastiani,[70a,70b] P. Seema,[24]

S. C. Seidel,[116] A. Seiden,[143] T. Seiss,[36] J. M. Seixas,[78b] G. Sekhniaidze,[67a] K. Sekhon,[103] S. J. Sekula,[41] N. Semprini-Cesari,[23b,23a] S. Sen,[47] S. Senkin,[37] C. Serfon,[130] L. Serin,[128] L. Serkin,[64a,64b] M. Sessa,[72a,72b] H. Severini,[124] T. Šfiligoj,[89] F. Sforza,[167] A. Sfyrla,[52] E. Shabalina,[51] J. D. Shahinian,[143] N. W. Shaikh,[43a,43b] L. Y. Shan,[15a] R. Shang,[170] J. T. Shank,[25] M. Shapiro,[18] A. S. Sharma,[1] A. Sharma,[131] P. B. Shatalov,[109] K. Shaw,[153] S. M. Shaw,[98] A. Shcherbakova,[134] Y. Shen,[124] N. Sherafati,[33] A. D. Sherman,[25] P. Sherwood,[92] L. Shi,[155,oo] S. Shimizu,[80] C. O. Shimmin,[180] M. Shimojima,[114] I. P. J. Shipsey,[131] S. Shirabe,[85] M. Shiyakova,[77] J. Shlomi,[177] A. Shmeleva,[108] D. Shoaleh Saadi,[107] M. J. Shochet,[36] S. Shojaii,[102] D. R. Shope,[124] S. Shrestha,[122] E. Shulga,[110] P. Sicho,[137] A. M. Sickles,[170] P. E. Sidebo,[151] E. Sideras Haddad,[32c] O. Sidiropoulou,[174] A. Sidoti,[23b,23a] F. Siegert,[46] Dj. Sijacki,[16] J. Silva,[136a] M. Silva Jr.,[178] M. V. Silva Oliveira,[78a] S. B. Silverstein,[43a] L. Simic,[77] S. Simion,[128] E. Simioni,[97] M. Simon,[97] R. Simoniello,[97] P. Sinervo,[164] N. B. Sinev,[127] M. Sioli,[23b,23a] G. Siragusa,[174] I. Siral,[103] S. Yu. Sivoklokov,[111] J. Sjölin,[43a,43b] M. B. Skinner,[87] P. Skubic,[124] M. Slater,[21] T. Slavicek,[138] M. Slawinska,[82] K. Sliwa,[167] R. Slovak,[139] V. Smakhtin,[177] B. H. Smart,[5] J. Smiesko,[28a] N. Smirnov,[110] S. Yu. Smirnov,[110] Y. Smirnov,[110] L. N. Smirnova,[111] O. Smirnova,[94] J. W. Smith,[51] M. N. K. Smith,[38] R. W. Smith,[38] M. Smizanska,[87] K. Smolek,[138] A. Smykiewicz,[82] A. A. Snesarev,[108] I. M. Snyder,[127] S. Snyder,[29] R. Sobie,[173,n] A. M. Soffa,[168] A. Soffer,[158] A. Søgaard,[48] D. A. Soh,[155] G. Sokhrannyi,[89] C. A. Solans Sanchez,[35] M. Solar,[138] E. Yu. Soldatov,[110] U. Soldevila,[171] A. A. Solodkov,[140] A. Soloshenko,[77] O. V. Solovyanov,[140] V. Solovyev,[134] P. Sommer,[146] H. Son,[167] W. Song,[141] A. Sopczak,[138] F. Sopkova,[28b] D. Sosa,[59b] C. L. Sotiropoulou,[69a,69b] S. Sottocornola,[68a,68b] R. Soualah,[64a,64c,pp] A. M. Soukharev,[120b,120a] D. South,[44] B. C. Sowden,[91] S. Spagnolo,[65a,65b] M. Spalla,[113] M. Spangenberg,[175] F. Spanò,[91] D. Sperlich,[19] F. Spettel,[113] T. M. Spieker,[59a] R. Spighi,[23b] G. Spigo,[35] L. A. Spiller,[102] D. P. Spiteri,[55] M. Spousta,[139] A. Stabile,[66a,66b] R. Stamen,[59a] S. Stamm,[19] E. Stanecka,[82] R. W. Stanek,[6] C. Stanescu,[72a] B. Stanislaus,[131] M. M. Stanitzki,[44] B. Stapf,[118] S. Stapnes,[130] E. A. Starchenko,[140] G. H. Stark,[36] J. Stark,[56] S. H Stark,[39] P. Staroba,[137] P. Starovoitov,[59a] S. Stärz,[35] R. Staszewski,[82] M. Stegler,[44] P. Steinberg,[29] B. Stelzer,[149] H. J. Stelzer,[35] O. Stelzer-Chilton,[165a] H. Stenzel,[54] T. J. Stevenson,[90] G. A. Stewart,[55] M. C. Stockton,[127] G. Stoicea,[27b] P. Stolte,[51] S. Stonjek,[113] A. Straessner,[46] J. Strandberg,[151] S. Strandberg,[43a,43b] M. Strauss,[124] P. Strizenec,[28b] R. Ströhmer,[174] D. M. Strom,[127] R. Stroynowski,[41] A. Strubig,[48] S. A. Stucci,[29] B. Stugu,[17] J. Stupak,[124] N. A. Styles,[44] D. Su,[150] J. Su,[135] S. Suchek,[59a] Y. Sugaya,[129] M. Suk,[138] V. V. Sulin,[108] D. M. S. Sultan,[52] S. Sultansoy,[4c] T. Sumida,[83] S. Sun,[103] X. Sun,[3] K. Suruliz,[153] C. J. E. Suster,[154] M. R. Sutton,[153] S. Suzuki,[79] M. Svatos,[137] M. Swiatlowski,[36] S. P. Swift,[2] A. Sydorenko,[97] I. Sykora,[28a] T. Sykora,[139] D. Ta,[97] K. Tackmann,[44,qq] J. Taenzer,[158] A. Taffard,[168] R. Tafirout,[165a] E. Tahirovic,[90] N. Taiblum,[158] H. Takai,[29] R. Takashima,[84] E. H. Takasugi,[113] K. Takeda,[80] T. Takeshita,[147] Y. Takubo,[79] M. Talby,[99] A. A. Talyshev,[120b,120a] J. Tanaka,[160] M. Tanaka,[162] R. Tanaka,[128] R. Tanioka,[80] B. B. Tannenwald,[122] S. Tapia Araya,[144b] S. Tapprogge,[97] A. Tarek Abouelfadl Mohamed,[132] S. Tarem,[157] G. Tarna,[27b,q] G. F. Tartarelli,[66a] P. Tas,[139] M. Tasevsky,[137] T. Tashiro,[83] E. Tassi,[40b,40a] A. Tavares Delgado,[136a,136b] Y. Tayalati,[34e] A. C. Taylor,[116] A. J. Taylor,[48] G. N. Taylor,[102] P. T. E. Taylor,[102] W. Taylor,[165b] A. S. Tee,[87] P. Teixeira-Dias,[91] H. Ten Kate,[35] P. K. Teng,[155] J. J. Teoh,[118] F. Tepel,[179] S. Terada,[79] K. Terashi,[160] J. Terron,[96] S. Terzo,[14] M. Testa,[49] R. J. Teuscher,[164,n] S. J. Thais,[180] T. Theveneaux-Pelzer,[44] F. Thiele,[39] D. W. Thomas,[91] J. P. Thomas,[21] A. S. Thompson,[55] P. D. Thompson,[21] L. A. Thomsen,[180] E. Thomson,[133] Y. Tian,[38] R. E. Ticse Torres,[51] V. O. Tikhomirov,[108,rr] Yu. A. Tikhonov,[120b,120a] S. Timoshenko,[110] P. Tipton,[180] S. Tisserant,[99] K. Todome,[162] S. Todorova-Nova,[5] S. Todt,[46] J. Tojo,[85] S. Tokár,[28a] K. Tokushuku,[79] E. Tolley,[122] K. G. Tomiwa,[32c] M. Tomoto,[115] L. Tompkins,[150,ff] K. Toms,[116] B. Tong,[57] P. Tornambe,[50] E. Torrence,[127] H. Torres,[46] E. Torró Pastor,[145] C. Tosciri,[131] J. Toth,[99,ss] F. Touchard,[99] D. R. Tovey,[146] C. J. Treado,[121] T. Trefzger,[174] F. Tresoldi,[153] A. Tricoli,[29] I. M. Trigger,[165a] S. Trincaz-Duvoid,[132] M. F. Tripiana,[14] W. Trischuk,[164] B. Trocmé,[56] A. Trofymov,[128] C. Troncon,[66a] M. Trovatelli,[173] F. Trovato,[153] L. Truong,[32b] M. Trzebinski,[82] A. Trzupek,[82] F. Tsai,[44] J. C-L. Tseng,[131] P. V. Tsiareshka,[105] N. Tsirintanis,[9] V. Tsiskaridze,[152] E. G. Tskhadadze,[156a] I. I. Tsukerman,[109] V. Tsulaia,[18] S. Tsuno,[79] D. Tsybychev,[152] Y. Tu,[61b] A. Tudorache,[27b] V. Tudorache,[27b] T. T. Tulbure,[27a] A. N. Tuna,[57] S. Turchikhin,[77] D. Turgeman,[177] I. Turk Cakir,[4b,tt] R. Turra,[66a] P. M. Tuts,[38] E. Tzovara,[97] G. Ucchielli,[23b,23a] I. Ueda,[79] M. Ughetto,[43a,43b] F. Ukegawa,[166] G. Unal,[35] A. Undrus,[29] G. Unel,[168] F. C. Ungaro,[102] Y. Unno,[79] K. Uno,[160] J. Urban,[28b] P. Urquijo,[102] P. Urrejola,[97] G. Usai,[8] J. Usui,[79] L. Vacavant,[99] V. Vacek,[138] B. Vachon,[101] K. O. H. Vadla,[130] A. Vaidya,[92] C. Valderanis,[112] E. Valdes Santurio,[43a,43b] M. Valente,[52] S. Valentinetti,[23b,23a] A. Valero,[171] L. Valéry,[44] R. A. Vallance,[21] A. Vallier,[5] J. A. Valls Ferrer,[171] T. R. Van Daalen,[14] W. Van Den Wollenberg,[118] H. Van der Graaf,[118] P. Van Gemmeren,[6] J. Van Nieuwkoop,[149] I. Van Vulpen,[118] M. Vanadia,[71a,71b] W. Vandelli,[35] A. Vaniachine,[163] P. Vankov,[118] R. Vari,[70a] E. W. Varnes,[7] C. Varni,[53b,53a] T. Varol,[41]

D. Varouchas,[128] K. E. Varvell,[154] G. A. Vasquez,[144b] J. G. Vasquez,[180] F. Vazeille,[37] D. Vazquez Furelos,[14] T. Vazquez Schroeder,[101] J. Veatch,[51] V. Vecchio,[72a,72b] L. M. Veloce,[164] F. Veloso,[136a,136c] S. Veneziano,[70a] A. Ventura,[65a,65b] M. Venturi,[173] N. Venturi,[35] V. Vercesi,[68a] M. Verducci,[72a,72b] C. M. Vergel Infante,[76] W. Verkerke,[118] A. T. Vermeulen,[118] J. C. Vermeulen,[118] M. C. Vetterli,[149,e] N. Viaux Maira,[144b] M. Vicente Barreto Pinto,[52] I. Vichou,[170,a] T. Vickey,[146] O. E. Vickey Boeriu,[146] G. H. A. Viehhauser,[131] S. Viel,[18] L. Vigani,[131] M. Villa,[23b,23a] M. Villaplana Perez,[66a,66b] E. Vilucchi,[49] M. G. Vincter,[33] V. B. Vinogradov,[77] A. Vishwakarma,[44] C. Vittori,[23b,23a] I. Vivarelli,[153] S. Vlachos,[10] M. Vogel,[179] P. Vokac,[138] G. Volpi,[14] S. E. von Buddenbrock,[32c] E. Von Toerne,[24] V. Vorobel,[139] K. Vorobev,[110] M. Vos,[171] J. H. Vossebeld,[88] N. Vranjes,[16] M. Vranjes Milosavljevic,[16] V. Vrba,[138] M. Vreeswijk,[118] R. Vuillermet,[35] I. Vukotic,[36] P. Wagner,[24] W. Wagner,[179] J. Wagner-Kuhr,[112] H. Wahlberg,[86] S. Wahrmund,[46] K. Wakamiya,[80] V. M. Walbrecht,[113] J. Walder,[87] R. Walker,[112] S. D. Walker,[91] W. Walkowiak,[148] V. Wallangen,[43a,43b] A. M. Wang,[57] C. Wang,[58b,q] F. Wang,[178] H. Wang,[18] H. Wang,[3] J. Wang,[154] J. Wang,[59b] P. Wang,[41] Q. Wang,[124] R.-J. Wang,[132] R. Wang,[58a] R. Wang,[6] S. M. Wang,[155] W. T. Wang,[58a] W. Wang,[15c,uu] W. X. Wang,[58a,uu] Y. Wang,[58a] Z. Wang,[58c] C. Wanotayaroj,[44] A. Warburton,[101] C. P. Ward,[31] D. R. Wardrope,[92] A. Washbrook,[48] P. M. Watkins,[21] A. T. Watson,[21] M. F. Watson,[21] G. Watts,[145] S. Watts,[98] B. M. Waugh,[92] A. F. Webb,[11] S. Webb,[97] C. Weber,[180] M. S. Weber,[20] S. A. Weber,[33] S. M. Weber,[59a] A. R. Weidberg,[131] B. Weinert,[63] J. Weingarten,[51] M. Weirich,[97] C. Weiser,[50] P. S. Wells,[35] T. Wenaus,[29] T. Wengler,[35] S. Wenig,[35] N. Wermes,[24] M. D. Werner,[76] P. Werner,[35] M. Wessels,[59a] T. D. Weston,[20] K. Whalen,[127] N. L. Whallon,[145] A. M. Wharton,[87] A. S. White,[103] A. White,[8] M. J. White,[1] R. White,[144b] D. Whiteson,[168] B. W. Whitmore,[87] F. J. Wickens,[141] W. Wiedenmann,[178] M. Wielers,[141] C. Wiglesworth,[39] L. A. M. Wiik-Fuchs,[50] A. Wildauer,[113] F. Wilk,[98] H. G. Wilkens,[35] L. J. Wilkins,[91] H. H. Williams,[133] S. Williams,[31] C. Willis,[104] S. Willocq,[100] J. A. Wilson,[21] I. Wingerter-Seez,[5] E. Winkels,[153] F. Winklmeier,[127] O. J. Winston,[153] B. T. Winter,[24] M. Wittgen,[150] M. Wobisch,[93] A. Wolf,[97] T. M. H. Wolf,[118] R. Wolff,[99] M. W. Wolter,[82] H. Wolters,[136a,136c] V. W. S. Wong,[172] N. L. Woods,[143] S. D. Worm,[21] B. K. Wosiek,[82] K. W. Woźniak,[82] K. Wraight,[55] M. Wu,[36] S. L. Wu,[178] X. Wu,[52] Y. Wu,[58a] T. R. Wyatt,[98] B. M. Wynne,[48] S. Xella,[39] Z. Xi,[103] L. Xia,[175] D. Xu,[15a] H. Xu,[58a] L. Xu,[29] T. Xu,[142] W. Xu,[103] B. Yabsley,[154] S. Yacoob,[32a] K. Yajima,[129] D. P. Yallup,[92] D. Yamaguchi,[162] Y. Yamaguchi,[162] A. Yamamoto,[79] T. Yamanaka,[160] F. Yamane,[80] M. Yamatani,[160] T. Yamazaki,[160] Y. Yamazaki,[80] Z. Yan,[25] H. J. Yang,[58c,58d] H. T. Yang,[18] S. Yang,[75] Y. Yang,[160] Z. Yang,[17] W-M. Yao,[18] Y. C. Yap,[44] Y. Yasu,[79] E. Yatsenko,[58c,58d] J. Ye,[41] S. Ye,[29] I. Yeletskikh,[77] E. Yigitbasi,[25] E. Yildirim,[97] K. Yorita,[176] K. Yoshihara,[133] C. J. S. Young,[35] C. Young,[150] J. Yu,[8] J. Yu,[76] X. Yue,[59a] S. P. Y. Yuen,[24] B. Zabinski,[82] G. Zacharis,[10] E. Zaffaroni,[52] R. Zaidan,[14] A. M. Zaitsev,[140,ll] N. Zakharchuk,[44] J. Zalieckas,[17] S. Zambito,[57] D. Zanzi,[35] D. R. Zaripovas,[55] S. V. Zeißner,[45] C. Zeitnitz,[179] G. Zemaityte,[131] J. C. Zeng,[170] Q. Zeng,[150] T. Ženiš,[28a] O. Zenin,[140] D. Zerwas,[128] M. Zgubič,[131] D. F. Zhang,[58b] D. Zhang,[103] F. Zhang,[178] G. Zhang,[58a] H. Zhang,[15c] J. Zhang,[6] L. Zhang,[15c] L. Zhang,[58a] M. Zhang,[170] P. Zhang,[15c] R. Zhang,[58a] R. Zhang,[24] X. Zhang,[58b] Y. Zhang,[15d] Z. Zhang,[128] X. Zhao,[41] Y. Zhao,[58b,128,y] Z. Zhao,[58a] A. Zhemchugov,[77] B. Zhou,[103] C. Zhou,[178] L. Zhou,[41] M. S. Zhou,[15d] M. Zhou,[152] N. Zhou,[58c] Y. Zhou,[7] C. G. Zhu,[58b] H. L. Zhu,[58a] H. Zhu,[15a] J. Zhu,[103] Y. Zhu,[58a] X. Zhuang,[15a] K. Zhukov,[108] V. Zhulanov,[120b,120a] A. Zibell,[174] D. Zieminska,[63] N. I. Zimine,[77] S. Zimmermann,[50] Z. Zinonos,[113] M. Zinser,[97] M. Ziolkowski,[148] L. Živković,[16] G. Zobernig,[178] A. Zoccoli,[23b,23a] K. Zoch,[51] T. G. Zorbas,[146] R. Zou,[36] M. Zur Nedden,[19] and L. Zwalinski[35]

(ATLAS Collaboration)

[1]*Department of Physics, University of Adelaide, Adelaide, Australia*
[2]*Physics Department, SUNY Albany, Albany, New York, USA*
[3]*Department of Physics, University of Alberta, Edmonton, Alberta, Canada*
[4a]*Department of Physics, Ankara University, Ankara, Turkey*
[4b]*Istanbul Aydin University, Istanbul, Turkey*
[4c]*Division of Physics, TOBB University of Economics and Technology, Ankara, Turkey*
[5]*LAPP, Université Grenoble Alpes, Université Savoie Mont Blanc, CNRS/IN2P3, Annecy, France*
[6]*High Energy Physics Division, Argonne National Laboratory, Argonne, Illinois, USA*
[7]*Department of Physics, University of Arizona, Tucson, Arizona, USA*
[8]*Department of Physics, University of Texas at Arlington, Arlington, Texas, USA*
[9]*Physics Department, National and Kapodistrian University of Athens, Athens, Greece*
[10]*Physics Department, National Technical University of Athens, Zografou, Greece*
[11]*Department of Physics, University of Texas at Austin, Austin, Texas, USA*
[12a]*Bahcesehir University, Faculty of Engineering and Natural Sciences, Istanbul, Turkey*

[12b]Istanbul Bilgi University, Faculty of Engineering and Natural Sciences, Istanbul, Turkey

[12c]Department of Physics, Bogazici University, Istanbul, Turkey

[12d]Department of Physics Engineering, Gaziantep University, Gaziantep, Turkey

[13]Institute of Physics, Azerbaijan Academy of Sciences, Baku, Azerbaijan

[14]Institut de Física d'Altes Energies (IFAE), Barcelona Institute of Science and Technology, Barcelona, Spain

[15a]Institute of High Energy Physics, Chinese Academy of Sciences, Beijing, China

[15b]Physics Department, Tsinghua University, Beijing, China

[15c]Department of Physics, Nanjing University, Nanjing, China

[15d]University of Chinese Academy of Science (UCAS), Beijing, China

[16]Institute of Physics, University of Belgrade, Belgrade, Serbia

[17]Department for Physics and Technology, University of Bergen, Bergen, Norway

[18]Physics Division, Lawrence Berkeley National Laboratory and University of California, Berkeley, California, USA

[19]Institut für Physik, Humboldt Universität zu Berlin, Berlin, Germany

[20]Albert Einstein Center for Fundamental Physics and Laboratory for High Energy Physics, University of Bern, Bern, Switzerland

[21]School of Physics and Astronomy, University of Birmingham, Birmingham, United Kingdom

[22]Centro de Investigaciónes, Universidad Antonio Nariño, Bogota, Colombia

[23a]Dipartimento di Fisica e Astronomia, Università di Bologna, Bologna, Italy

[23b]INFN Sezione di Bologna, Italy

[24]Physikalisches Institut, Universität Bonn, Bonn, Germany

[25]Department of Physics, Boston University, Boston, Massachusetts, USA

[26]Department of Physics, Brandeis University, Waltham, Massachusetts, USA

[27a]Transilvania University of Brasov, Brasov, Romania

[27b]Horia Hulubei National Institute of Physics and Nuclear Engineering, Bucharest, Romania

[27c]Department of Physics, Alexandru Ioan Cuza University of Iasi, Iasi, Romania

[27d]National Institute for Research and Development of Isotopic and Molecular Technologies, Physics Department, Cluj-Napoca, Romania

[27e]University Politehnica Bucharest, Bucharest, Romania

[27f]West University in Timisoara, Timisoara, Romania

[28a]Faculty of Mathematics, Physics and Informatics, Comenius University, Bratislava, Slovak Republic

[28b]Department of Subnuclear Physics, Institute of Experimental Physics of the Slovak Academy of Sciences, Kosice, Slovak Republic

[29]Physics Department, Brookhaven National Laboratory, Upton, New York, USA

[30]Departamento de Física, Universidad de Buenos Aires, Buenos Aires, Argentina

[31]Cavendish Laboratory, University of Cambridge, Cambridge, United Kingdom

[32a]Department of Physics, University of Cape Town, Cape Town, South Africa

[32b]Department of Mechanical Engineering Science, University of Johannesburg, Johannesburg, South Africa

[32c]School of Physics, University of the Witwatersrand, Johannesburg, South Africa

[33]Department of Physics, Carleton University, Ottawa, Ontario, Canada

[34a]Faculté des Sciences Ain Chock, Réseau Universitaire de Physique des Hautes Energies - Université Hassan II, Casablanca, Morocco

[34b]Centre National de l'Energie des Sciences Techniques Nucleaires (CNESTEN), Rabat, Morocco

[34c]Faculté des Sciences Semlalia, Université Cadi Ayyad, LPHEA-Marrakech, Morocco

[34d]Faculté des Sciences, Université Mohamed Premier and LPTPM, Oujda, Morocco

[34e]Faculté des sciences, Université Mohammed V, Rabat, Morocco

[35]CERN, Geneva, Switzerland

[36]Enrico Fermi Institute, University of Chicago, Chicago, Illinois, USA

[37]LPC, Université Clermont Auvergne, CNRS/IN2P3, Clermont-Ferrand, France

[38]Nevis Laboratory, Columbia University, Irvington, New York, USA

[39]Niels Bohr Institute, University of Copenhagen, Copenhagen, Denmark

[40a]Dipartimento di Fisica, Università della Calabria, Rende, Italy

[40b]INFN Gruppo Collegato di Cosenza, Laboratori Nazionali di Frascati, Italy

[41]Physics Department, Southern Methodist University, Dallas, Texas, USA

[42]Physics Department, University of Texas at Dallas, Richardson, Texas, USA

[43a]Department of Physics, Stockholm University, Sweden

[43b]Oskar Klein Centre, Stockholm, Sweden

[44]Deutsches Elektronen-Synchrotron DESY, Hamburg and Zeuthen, Germany

[45]Lehrstuhl für Experimentelle Physik IV, Technische Universität Dortmund, Dortmund, Germany

[46]Institut für Kern- und Teilchenphysik, Technische Universität Dresden, Dresden, Germany

[47]Department of Physics, Duke University, Durham, North Carolina, USA

[48]SUPA - School of Physics and Astronomy, University of Edinburgh, Edinburgh, United Kingdom

[49]INFN e Laboratori Nazionali di Frascati, Frascati, Italy

[50]Physikalisches Institut, Albert-Ludwigs-Universität Freiburg, Freiburg, Germany

[51]II. Physikalisches Institut, Georg-August-Universität Göttingen, Göttingen, Germany

[52]Département de Physique Nucléaire et Corpusculaire, Université de Genève, Genève, Switzerland

[53a]Dipartimento di Fisica, Università di Genova, Genova, Italy

[53b]INFN Sezione di Genova, Italy

[54]II. Physikalisches Institut, Justus-Liebig-Universität Giessen, Giessen, Germany

[55]SUPA - School of Physics and Astronomy, University of Glasgow, Glasgow, United Kingdom

[56]LPSC, Université Grenoble Alpes, CNRS/IN2P3, Grenoble INP, Grenoble, France

[57]Laboratory for Particle Physics and Cosmology, Harvard University, Cambridge, Massachusetts, USA

[58a]Department of Modern Physics and State Key Laboratory of Particle Detection and Electronics,
University of Science and Technology of China, Hefei, China

[58b]Institute of Frontier and Interdisciplinary Science and Key Laboratory of Particle Physics
and Particle Irradiation (MOE), Shandong University, Qingdao, China

[58c]School of Physics and Astronomy, Shanghai Jiao Tong University,
KLPPAC-MoE, SKLPPC, Shanghai, China

[58d]Tsung-Dao Lee Institute, Shanghai, China

[59a]Kirchhoff-Institut für Physik, Ruprecht-Karls-Universität Heidelberg, Heidelberg, Germany

[59b]Physikalisches Institut, Ruprecht-Karls-Universität Heidelberg, Heidelberg, Germany

[60]Faculty of Applied Information Science, Hiroshima Institute of Technology, Hiroshima, Japan

[61a]Department of Physics, Chinese University of Hong Kong, Shatin, N.T., Hong Kong, China

[61b]Department of Physics, University of Hong Kong, Hong Kong, China

[61c]Department of Physics and Institute for Advanced Study, Hong Kong University of Science and
Technology, Clear Water Bay, Kowloon, Hong Kong, China

[62]Department of Physics, National Tsing Hua University, Hsinchu, Taiwan

[63]Department of Physics, Indiana University, Bloomington, Indiana, USA

[64a]INFN Gruppo Collegato di Udine, Sezione di Trieste, Udine, Italy

[64b]ICTP, Trieste, Italy

[64c]Dipartimento di Chimica, Fisica e Ambiente, Università di Udine, Udine, Italy

[65a]INFN Sezione di Lecce, Italy

[65b]Dipartimento di Matematica e Fisica, Università del Salento, Lecce, Italy

[66a]INFN Sezione di Milano, Italy

[66b]Dipartimento di Fisica, Università di Milano, Milano, Italy

[67a]INFN Sezione di Napoli, Italy

[67b]Dipartimento di Fisica, Università di Napoli, Napoli, Italy

[68a]INFN Sezione di Pavia, Italy

[68b]Dipartimento di Fisica, Università di Pavia, Pavia, Italy

[69a]INFN Sezione di Pisa, Italy

[69b]Dipartimento di Fisica E. Fermi, Università di Pisa, Pisa, Italy

[70a]INFN Sezione di Roma, Italy

[70b]Dipartimento di Fisica, Sapienza Università di Roma, Roma, Italy

[71a]INFN Sezione di Roma Tor Vergata, Italy

[71b]Dipartimento di Fisica, Università di Roma Tor Vergata, Roma, Italy

[72a]INFN Sezione di Roma Tre, Italy

[72b]Dipartimento di Matematica e Fisica, Università Roma Tre, Roma, Italy

[73a]INFN-TIFPA, Italy

[73b]Università degli Studi di Trento, Trento, Italy

[74]Institut für Astro- und Teilchenphysik, Leopold-Franzens-Universität, Innsbruck, Austria

[75]University of Iowa, Iowa City, Iowa, USA

[76]Department of Physics and Astronomy, Iowa State University, Ames, Iowa, USA

[77]Joint Institute for Nuclear Research, Dubna, Russia

[78a]Departamento de Engenharia Elétrica, Universidade Federal de Juiz de Fora (UFJF),
Juiz de Fora, Brazil

[78b]Universidade Federal do Rio De Janeiro COPPE/EE/IF, Rio de Janeiro, Brazil

[78c]Universidade Federal de São João del Rei (UFSJ), São João del Rei, Brazil

[78d]Instituto de Física, Universidade de São Paulo, São Paulo, Brazil

[79]KEK, High Energy Accelerator Research Organization, Tsukuba, Japan

[80]Graduate School of Science, Kobe University, Kobe, Japan

[81a]AGH University of Science and Technology, Faculty of Physics and Applied Computer Science,
Krakow, Poland

[81b]Marian Smoluchowski Institute of Physics, Jagiellonian University, Krakow, Poland

[82]Institute of Nuclear Physics Polish Academy of Sciences, Krakow, Poland

[83]Faculty of Science, Kyoto University, Kyoto, Japan

[84]Kyoto University of Education, Kyoto, Japan

[85]Research Center for Advanced Particle Physics and Department of Physics,
Kyushu University, Fukuoka, Japan

[86]Instituto de Física La Plata, Universidad Nacional de La Plata and CONICET, La Plata, Argentina

[87]Physics Department, Lancaster University, Lancaster, United Kingdom

[88]Oliver Lodge Laboratory, University of Liverpool, Liverpool, United Kingdom

[89]Department of Experimental Particle Physics, Jožef Stefan Institute and Department of Physics,
University of Ljubljana, Ljubljana, Slovenia

[90]School of Physics and Astronomy, Queen Mary University of London, London, United Kingdom

[91]Department of Physics, Royal Holloway University of London, Egham, United Kingdom

[92]Department of Physics and Astronomy, University College London, London, United Kingdom

[93]Louisiana Tech University, Ruston, Louisiana, USA

[94]Fysiska institutionen, Lunds universitet, Lund, Sweden

[95]Centre de Calcul de l'Institut National de Physique Nucléaire et de Physique des Particules (IN2P3),
Villeurbanne, France

[96]Departamento de Física Teorica C-15 and CIAFF, Universidad Autónoma de Madrid, Madrid, Spain

[97]Institut für Physik, Universität Mainz, Mainz, Germany

[98]School of Physics and Astronomy, University of Manchester, Manchester, United Kingdom

[99]CPPM, Aix-Marseille Université, CNRS/IN2P3, Marseille, France

[100]Department of Physics, University of Massachusetts, Amherst, Massachusetts, USA

[101]Department of Physics, McGill University, Montreal, Quebec, Canada

[102]School of Physics, University of Melbourne, Victoria, Australia

[103]Department of Physics, University of Michigan, Ann Arbor, Michigan, USA

[104]Department of Physics and Astronomy, Michigan State University, East Lansing, Michigan, USA

[105]B.I. Stepanov Institute of Physics, National Academy of Sciences of Belarus, Minsk, Belarus

[106]Research Institute for Nuclear Problems of Byelorussian State University, Minsk, Belarus

[107]Group of Particle Physics, University of Montreal, Montreal, Quebec, Canada

[108]P.N. Lebedev Physical Institute of the Russian Academy of Sciences, Moscow, Russia

[109]Institute for Theoretical and Experimental Physics (ITEP), Moscow, Russia

[110]National Research Nuclear University MEPhI, Moscow, Russia

[111]D.V. Skobeltsyn Institute of Nuclear Physics,
M.V. Lomonosov Moscow State University, Moscow, Russia

[112]Fakultät für Physik, Ludwig-Maximilians-Universität München, München, Germany

[113]Max-Planck-Institut für Physik (Werner-Heisenberg-Institut), München, Germany

[114]Nagasaki Institute of Applied Science, Nagasaki, Japan

[115]Graduate School of Science and Kobayashi-Maskawa Institute, Nagoya University, Nagoya, Japan

[116]Department of Physics and Astronomy, University of New Mexico, Albuquerque, New Mexico, USA

[117]Institute for Mathematics, Astrophysics and Particle Physics, Radboud University Nijmegen/Nikhef,
Nijmegen, Netherlands

[118]Nikhef National Institute for Subatomic Physics and University of Amsterdam, Amsterdam, Netherlands

[119]Department of Physics, Northern Illinois University, DeKalb, Illinois, USA

[120a]Budker Institute of Nuclear Physics, SB RAS, Novosibirsk, Russia

[120b]Novosibirsk State University Novosibirsk, Russia

[121]Department of Physics, New York University, New York, New York, USA

[122]The Ohio State University, Columbus, Ohio, USA

[123]Faculty of Science, Okayama University, Okayama, Japan

[124]Homer L. Dodge Department of Physics and Astronomy, University of Oklahoma,
Norman, Oklahoma, USA

[125]Department of Physics, Oklahoma State University, Stillwater, Oklahoma, USA

[126]Palacký University, RCPTM, Joint Laboratory of Optics, Olomouc, Czech Republic

[127]Center for High Energy Physics, University of Oregon, Eugene, Oregon, USA

[128]LAL, Université Paris-Sud, CNRS/IN2P3, Université Paris-Saclay, Orsay, France

[129]Graduate School of Science, Osaka University, Osaka, Japan

[130]Department of Physics, University of Oslo, Oslo, Norway

[131]Department of Physics, Oxford University, Oxford, United Kingdom

[132]LPNHE, Sorbonne Université, Paris Diderot Sorbonne Paris Cité, CNRS/IN2P3, Paris, France

[133]Department of Physics, University of Pennsylvania, Philadelphia, Pennsylvania, USA

[134]Konstantinov Nuclear Physics Institute of National Research Centre "Kurchatov Institute,"
PNPI, St. Petersburg, Russia

[135]Department of Physics and Astronomy, University of Pittsburgh, Pittsburgh, Pennsylvania, USA

[136a]Laboratório de Instrumentação e Física Experimental de Partículas - LIP, Portugal

[136b]Departamento de Física, Faculdade de Ciências, Universidade de Lisboa, Lisboa, Portugal

[136c]Departamento de Física, Universidade de Coimbra, Coimbra, Portugal

[136d]Centro de Física Nuclear da Universidade de Lisboa, Lisboa, Portugal

[136e]Departamento de Física, Universidade do Minho, Braga, Portugal

[136f]Departamento de Física Teorica y del Cosmos, Universidad de Granada, Granada (Spain), Spain

[136g]Dep Física and CEFITEC of Faculdade de Ciências e Tecnologia,
Universidade Nova de Lisboa, Caparica, Portugal

[137]Institute of Physics, Academy of Sciences of the Czech Republic, Prague, Czech Republic

[138]Czech Technical University in Prague, Prague, Czech Republic

[139]Charles University, Faculty of Mathematics and Physics, Prague, Czech Republic

[140]State Research Center Institute for High Energy Physics, NRC KI, Protvino, Russia

[141]Particle Physics Department, Rutherford Appleton Laboratory, Didcot, United Kingdom

[142]IRFU, CEA, Université Paris-Saclay, Gif-sur-Yvette, France

[143]Santa Cruz Institute for Particle Physics, University of California Santa Cruz,
Santa Cruz, California, USA

[144a]Departamento de Física, Pontificia Universidad Católica de Chile, Santiago, Chile

[144b]Departamento de Física, Universidad Técnica Federico Santa María, Valparaíso, Chile

[145]Department of Physics, University of Washington, Seattle, Washington, USA

[146]Department of Physics and Astronomy, University of Sheffield, Sheffield, United Kingdom

[147]Department of Physics, Shinshu University, Nagano, Japan

[148]Department Physik, Universität Siegen, Siegen, Germany

[149]Department of Physics, Simon Fraser University, Burnaby, British Columbia, Canada

[150]SLAC National Accelerator Laboratory, Stanford, California, USA

[151]Physics Department, Royal Institute of Technology, Stockholm, Sweden

[152]Departments of Physics and Astronomy, Stony Brook University, Stony Brook, New York, USA

[153]Department of Physics and Astronomy, University of Sussex, Brighton, United Kingdom

[154]School of Physics, University of Sydney, Sydney, Australia

[155]Institute of Physics, Academia Sinica, Taipei, Taiwan

[156a]E. Andronikashvili Institute of Physics, Iv. Javakhishvili Tbilisi State University, Tbilisi, Georgia

[156b]High Energy Physics Institute, Tbilisi State University, Tbilisi, Georgia

[157]Department of Physics, Technion, Israel Institute of Technology, Haifa, Israel

[158]Raymond and Beverly Sackler School of Physics and Astronomy, Tel Aviv University, Tel Aviv, Israel

[159]Department of Physics, Aristotle University of Thessaloniki, Thessaloniki, Greece

[160]International Center for Elementary Particle Physics and Department of Physics,
University of Tokyo, Tokyo, Japan

[161]Graduate School of Science and Technology, Tokyo Metropolitan University, Tokyo, Japan

[162]Department of Physics, Tokyo Institute of Technology, Tokyo, Japan

[163]Tomsk State University, Tomsk, Russia

[164]Department of Physics, University of Toronto, Toronto, Ontario, Canada

[165a]TRIUMF, Vancouver, British Columbia, Canada

[165b]Department of Physics and Astronomy, York University, Toronto, Ontario, Canada

[166]Division of Physics and Tomonaga Center for the History of the Universe, Faculty of Pure and Applied
Sciences, University of Tsukuba, Tsukuba, Japan

[167]Department of Physics and Astronomy, Tufts University, Medford, Massachusetts, USA

[168]Department of Physics and Astronomy, University of California Irvine, Irvine, California, USA

[169]Department of Physics and Astronomy, University of Uppsala, Uppsala, Sweden

[170]Department of Physics, University of Illinois, Urbana, Illinois, USA

[171]Instituto de Física Corpuscular (IFIC), Centro Mixto Universidad de Valencia - CSIC, Valencia, Spain

[172]Department of Physics, University of British Columbia, Vancouver, British Columbia, Canada

[173]Department of Physics and Astronomy, University of Victoria, Victoria, British Columbia, Canada

[174]Fakultät für Physik und Astronomie, Julius-Maximilians-Universität Würzburg, Würzburg, Germany

[175]Department of Physics, University of Warwick, Coventry, United Kingdom

[176]*Waseda University, Tokyo, Japan*
[177]*Department of Particle Physics, Weizmann Institute of Science, Rehovot, Israel*
[178]*Department of Physics, University of Wisconsin, Madison, Wisconsin, USA*
[179]*Fakultät für Mathematik und Naturwissenschaften, Fachgruppe Physik,*
Bergische Universität Wuppertal, Wuppertal, Germany
[180]*Department of Physics, Yale University, New Haven, Connecticut, USA*
[181]*Yerevan Physics Institute, Yerevan, Armenia*

[a]Deceased.
[b]Also at Department of Physics, King's College London, London, United Kingdom.
[c]Also at Istanbul University, Department of Physics, Istanbul, Turkey.
[d]Also at Institute of Physics, Azerbaijan Academy of Sciences, Baku, Azerbaijan.
[e]Also at TRIUMF, Vancouver, British Columbia, Canada.
[f]Also at Department of Physics and Astronomy, University of Louisville, Louisville, Kentucky, USA.
[g]Also at Department of Physics, California State University, Fresno, California, USA.
[h]Also at Department of Physics, University of Fribourg, Fribourg, Switzerland.
[i]Also at II. Physikalisches Institut, Georg-August-Universität Göttingen, Göttingen, Germany.
[j]Also at Departament de Fisica de la Universitat Autonoma de Barcelona, Barcelona, Spain.
[k]Also at Tomsk State University, Tomsk, and Moscow Institute of Physics and Technology State University, Dolgoprudny, Russia.
[l]Also at The Collaborative Innovation Center of Quantum Matter (CICQM), Beijing, China.
[m]Also at Universita di Napoli Parthenope, Napoli, Italy.
[n]Also at Institute of Particle Physics (IPP), Canada.
[o]Also at Dipartimento di Fisica E. Fermi, Università di Pisa, Pisa, Italy.
[p]Also at Horia Hulubei National Institute of Physics and Nuclear Engineering, Bucharest, Romania.
[q]Also at CPPM, Aix-Marseille Université, CNRS/IN2P3, Marseille, France.
[r]Also at Department of Physics, St. Petersburg State Polytechnical University, St. Petersburg, Russia.
[s]Also at Borough of Manhattan Community College, City University of New York, New York, USA.
[t]Also at Department of Financial and Management Engineering, University of the Aegean, Chios, Greece.
[u]Also at Centre for High Performance Computing, CSIR Campus, Rosebank, Cape Town, South Africa.
[v]Also at Louisiana Tech University, Ruston, Louisiana, USA.
[w]Also at Institucio Catalana de Recerca i Estudis Avancats, ICREA, Barcelona, Spain.
[x]Also at Department of Physics, University of Michigan, Ann Arbor, Michigan, USA.
[y]Also at LAL, Université Paris-Sud, CNRS/IN2P3, Université Paris-Saclay, Orsay, France.
[z]Also at Graduate School of Science, Osaka University, Osaka, Japan.
[aa]Also at Physikalisches Institut, Albert-Ludwigs-Universität Freiburg, Freiburg, Germany.
[bb]Also at Institute for Mathematics, Astrophysics and Particle Physics, Radboud University Nijmegen/Nikhef, Nijmegen, Netherlands.
[cc]Also at Near East University, Nicosia, North Cyprus, Mersin, Turkey.
[dd]Also at Institute of Theoretical Physics, Ilia State University, Tbilisi, Georgia.
[ee]Also at CERN, Geneva, Switzerland.
[ff]Also at Department of Physics, Stanford University, USA.
[gg]Also at Manhattan College, New York, New York, USA.
[hh]Also at Hellenic Open University, Patras, Greece.
[ii]Also at The City College of New York, New York, New York, USA.
[jj]Also at Departamento de Física Teorica y del Cosmos, Universidad de Granada, Granada (Spain), Spain.
[kk]Also at Department of Physics, California State University, Sacramento, California, USA.
[ll]Also at Moscow Institute of Physics and Technology State University, Dolgoprudny, Russia.
[mm]Also at Département de Physique Nucléaire et Corpusculaire, Université de Genève, Genève, Switzerland.
[nn]Also at Department of Physics and Astronomy, University of Sheffield, Sheffield, United Kingdom.
[oo]Also at School of Physics, Sun Yat-sen University, Guangzhou, China.
[pp]Also at Department of Applied Physics and Astronomy, University of Sharjah, Sharjah, United Arab Emirates.
[qq]Also at Institut für Experimentalphysik, Universität Hamburg, Hamburg, Germany.
[rr]Also at National Research Nuclear University MEPhI, Moscow, Russia.
[ss]Also at Institute for Particle and Nuclear Physics, Wigner Research Centre for Physics, Budapest, Hungary.
[tt]Also at Giresun University, Faculty of Engineering, Giresun, Turkey.
[uu]Also at Institute of Physics, Academia Sinica, Taipei, Taiwan.